Automatic start up of ESP-lifted wells

Title: **Automatic start up of ESP-lifted wells**		
Document no. :	Contract no.:	Project:

Classification: **Internal**	Distribution: **Corporate Statoil**
Expiry date:	Status **Final**

Distribution date:	Rev. no.:	Copy no.:

Author(s)/Source(s): **David Skålid Amundsen, Wenjing Zhou, Arne Scherrer**	
Subjects: **Report on model, simulation and program**	
Remarks:	
Valid from:	Updated:
Responsible publisher:	Authority to approve deviations:

Techn. responsible	Techn. responsible (Name):	Date/Signature:
Responsible (Organisation	Responsible (Name):	Date/Signature:
Recommended (Organisation	Recommended (Name):	Date/Signature:
Approved by (Organisation	Approved by (Name):	Date/Signature:

Abstract

In this report, the work on modelling and controlling ESP lifted wells done by three summer students in 2010 are presented. Both a static and a dynamic models will be developed for different levels of complexity. The simplest model is implemented for both one single well, and for an arbitrary number of wells, and the more complex model is developed for one single well. The implementation of the models are presented and discussed, and the static model is compared to field data. Also, the results from the simulations are presented. Simple controllers are implemented and discussed.

Our work shows that a fairly simple model may be enough in order to get results on the accuracy scale needed, but the simplest model may not be desirable because of low calculation speed due to numerical details. A more complex model with a possible low spatial resolution that is both faster and more accurate will be presented and discussed.

The comparison of the simulation results to the field data shows partial agreement. This is mainly due to limited data quality and quantity.

The control developed, PI controllers for the ESPs and the production chokes with implemented quantizers, appears to produce the desired behaviour. That is, to keep the ESPs within the operational regimes in order not to damage the ESPs.

Table of contents

1 Introduction[1]

In a production system without artificial lift, reservoir pressure is sufficiently high to make the oil rise naturally to the surface. In this case the reservoir pressure is higher than the hydrostatic pressure, which is determined by the density of the produced liquid and the depth of the well. Sometimes the reservoir pressure is lower than the hydrostatic pressure needed to produce oil. This happens, for example, in depleted reservoirs, in wells producing high density liquid (e.g. heavy oil or liquid or fluid of a high water cut). In this case wells should be equipped with artificial lift systems that provide the necessary pressure increase to assure production. In addition, artificial lift systems can be used to boost production in naturally flowing wells.

In this project we consider an artificial lift system based on electrical submersible pumps (ESP). These are multistage centrifugal pumps deployed in wells to increase the lifting pressure. A simple scheme of such a production system equipped with an ESP-based artificial lift system is depicted in Figure 1.

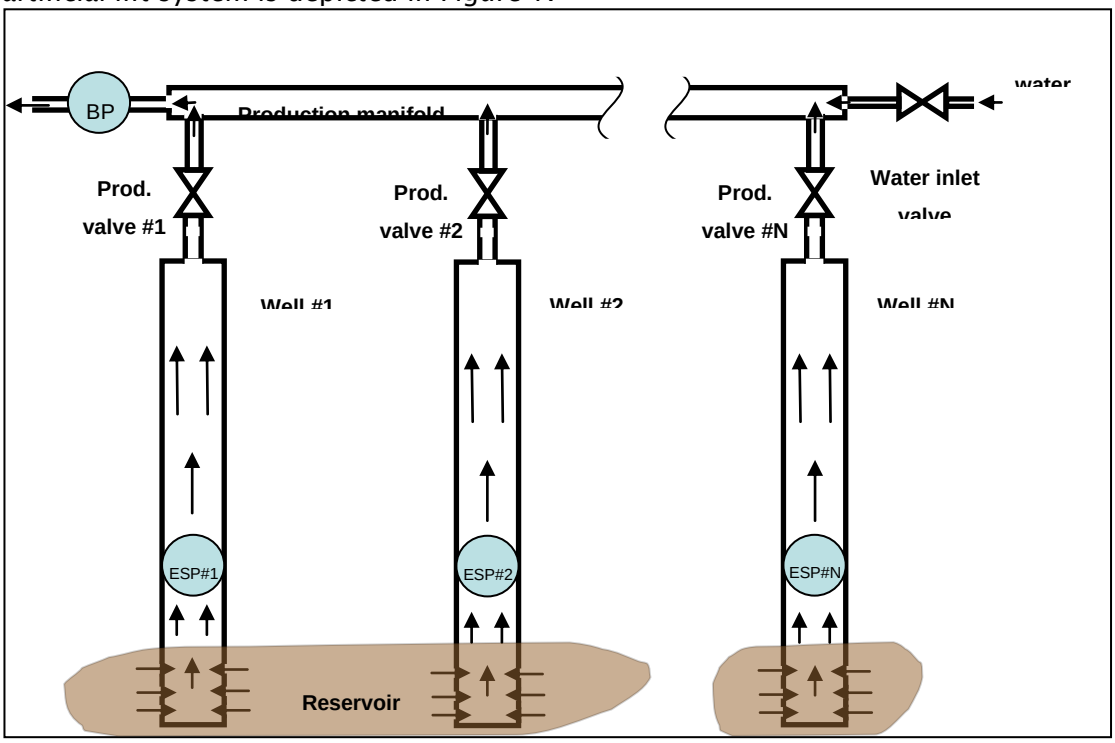

Figure 1: Sketch of a system consisting of N wells connected to a common manifold.

[1] Originally written by Alexy Pavlov in the definition of this summer project, slightly changed and expanded.

In this scheme, several wells equipped with ESPs are connected through production valves to a production manifold. An additional inlet to the production manifold supplies water, which mixes with the produced liquid in the production manifold. Then this mixture of oil and water flows into a production line through a booster pump. In this configuration, ESPs are needed to provide sufficient lift to rise oil from the reservoir to the production manifold located at the seabed. The additional water supply is needed to provide sufficient viscosity properties of the mixture to be risen in the production line (if the mixture has high viscosity, it is difficult to transport it through the production line, and in some cases adding water can reduce the viscosity of the mixture). The production booster pump is needed to guarantee necessary lift for rising the mixture from the seabed to the sea surface (platform or FPSO).

In this system several components can be controlled. In particular, ESPs are controlled through variable frequency (speed) drives VFD (or VSD) by supplying AC current to the pumps with varying frequency. This frequency determines the lift produced by the pump (in fact, it, together with the load on the pump determines the rotational velocity of the pump, which, in turn, determines the differential pressure of the pump – the pressure added by the pump). The production booster pump (BP) is controlled in the same way. Openings of the production valves and the water inlet valve are also controlled. All these pumps and valves should be controlled in a coordinated manner to ensure safe operation of the equipment within its operational envelopes on the one hand, and to maximize oil production, on the other hand.

Safe operation of equipment includes, among others, operation of ESPs strictly within their operational envelope. This envelope is determined by several factors. For example, ESPs are cooled down by the flow going through the pump. If an ESP is operated at high frequency (e.g. high power), but with low flow, this will result in an ESP failure. On the other hand, very high flow may result in cavitation and mechanical damage of the pump. Too high suction power of the ESP may result in a high amount of sand at the pump intake, which may also result in a mechanical damage or in reduced life-time of the pump. Operating the pump with the reverse flow also leads to damaging the pump. At the moment, control of ESP-lifted wells (through controlling ESPs and valves) is performed manually. As follows from the available statistics on ESP failures, around 23% of all ESP failures are due to wrong operation of the system (i.e. operating the pumps outside their operational envelopes). By reducing the human factor (erroneous actions of operators), one can reduce this high percentage and thus increase average ESP life-time, which nowadays is around 3 years. It should be mentioned that increasing ESP life-time has direct economical consequences since the costs for fixing an ESP are very high. Apart from direct costs for fixing or replacing the pump itself, these costs include losses due to non-production time due to tripping the ESP and tubing out of the well and deploying a new ESP. Taking into account the increasing number of fields with ESP lifted wells, improvements of ESP operations that lead to longer ESP life-time will be economically profitable.

When the system is operated in a steady-state condition (all state variables of the system as well as inputs – environmental or operator-manipulated – are constant), control inputs corresponding to optimal operation of ESPs and valves can be computed offline in advance. Then they can be used in a form of a look-up table. Some of the most challenging operations, from an operator point of view, are operations of transition from one steady-state to another steady-state, which occur, for example, during start-up and shut-down of one or several wells. In the start-up case, the initial steady-state corresponds to the situation when all ESPs of the wells to be started are shut down and the corresponding production valves are closed. All remaining wells are producing with a desired production rate (which implies that their ESPs and valves are operated at some optimal regimes corresponding to existing conditions). The final steady-state corresponds to the situation when all wells, including the ones to be started, are producing at their desired production rates, with their control inputs (frequencies for pumps and valve openings) being chosen from the look-up table described above. Transition between the initial and final steady-states needs to satisfy all constraints corresponding to safe operation of the hardware. At the same time, the transition should be done in a desired time frame, e.g. as fast as possible. Another example of a transitional operation corresponds to the case when one of the valves in the overall system is closed/opened manually, for example in an emergency shut down. This requires fast adaptation of operation of the remaining valves and ESPs to the new operational conditions to keep the overall system in a safe operational envelope and, preferably, as close to an optimal regime, as possible.

At the moment these transitional operations are performed manually by following procedures predefined beforehand, i.e. offline. On the one hand, such procedures are rather conservative since they do not take into account measurements available online. On the other hand, manual operation increases the probability of erroneous operation due to human factor, especially in the case when an operator needs to start up several wells simultaneously and thus needs to monitor a number of parameters corresponding to different wells. If an ESP goes out of its operational envelope, it needs to be shut down (to save it from damage). Each shut down of an ESP reduces its life-time. Moreover, there is a constraint that a certain period should pass before another attempt for start-up can be taken. Thus each failure in start up of a well leads to increased non-production time.

The factors described above indicate that there is a need for automation of transitional operations in ESP-lifted wells, including their start-up and shut-down. An automatic controller for these operations can take into account in a systematic manner 1) all measurements and data available online, 2) operational constraints and 3) available process models. Moreover, automatic control can be employed simultaneously for a number of wells connected to the same production unit. By taking into account all the available online information and by processing it in a comprehensive way, automatic controller can achieve safer and more optimal operation of the system compared to manual operation. The main consequences of employing automatic control include

reduced non-production time related to start-up and shut-down of ESP-lifted wells and increased life-time of ESPs, which, in turn, also leads to reduction of non-production time.

In this project a first prototype of such a described automated control system was set up. Starting from scratch also the underlying physical models had to be developed and implemented in order to provide a toolbox for more advanced controller design. In the following sections of this report the simple and complex model are derived. The implementation of these models is presented and discussed and their steady states are compared to field data. The results from the simulations are presented and the control system is described and its application discussed.

2 Theory

2.1 Fluid flow fundamentals

Since water and oil behave like Newtonian fluids it is possible to apply the theory of fluid mechanics. The system is described by the following fundamental principles.

- Equation of State
- Continuity equation
- Momentum equation
- Conservation of Energy

Additionally the viscosity and its dependence on pressure, temperature and water cut can be considered.

2.2 Overall assumptions

The following assumptions were made for the modelling of the system:

1. One dimension and homogeneous cross sectional conditions:
   The whole system is reduced to one dimension applying Reynolds' time averaging concept, i.e. time averaging the fluctuations due to turbulences. Accordingly, cross sectional dependencies are not taken into account explicitly. Though by considering cross sectional averaged values they are taken into account implicitly. In particular head losses due to turbulence cannot be considered directly and have to be treated separately in a friction model.
2. Single phase flow:
   The whole system is considered to be fully saturated with a single phase fluid. Actually this fluid consists of oil, water and gas which is dissolved to a certain degree depending on the temperature and pressure conditions. Despite that it is convenient to model a single phase flow for the following reasons: Between the reservoir and the pump the hydrostatic pressure is high enough for the gas to stay dissolved. It is then separated before the pump so that in and after the pump the bubble point is fairly low and should not be reached due to the operating restrictions. Concerning the water-oil-solution it is possible to model the dominating effects by properties of a single phase fluid, e.g. viscosity and density dependence of the water cut.
   During the start-up or shut-down or for certain pressure conditions this assumption does not hold. This will be discussed in the section on negative pressures and simulation of start-up.
3. Incompressibility in momentum equation:
   Referring to [1] a flow can be termed incompressible for Mach numbers less than 0.3. Therefore it is possible to use the simplified Navier-Stokes-Equation for incompressible fluids. However for time evolution a pressure differential equation is needed. It is therefore convenient to take compressibility into account in the continuity equation [2].
4. Isothermal conditions:

All temperature dependencies are neglected even though significant temperature gradients may exist. This can be justified by the fact that the thermal expansion coefficients are very small and also the temperature dependency of the viscosity is negligible compared to other effects as e.g. the water cut or the amount of dissolved gas.

5. Equation of state:
As for the equation of state a linear behaviour around the reference point is assumed since the changes in density as a function of pressure and temperature are very small for a liquid. Due to the isothermal assumption the temperature dependency is omitted.

2.3 Continuity equation

The continuity equation in form of Eulerian derivatives is given by

$$\frac{\partial \rho}{\partial t} + \nabla \cdot (\rho \cdot \vec{v}) = 0$$

Here ρ is the density and $\vec{v}$ is the velocity field describing the motion of the fluid.

2.4 Momentum equation

According to the assumptions made, the momentum equation for the time and cross section averaged flow variables is given by the Navier-Stokes-Equation for an incompressible fluid [1,p. 304]:

$$\rho \cdot \frac{dv}{dt} = -\frac{\partial p}{\partial x} + \mu \frac{\partial \tau}{\partial r} + \rho \cdot g \frac{\partial h}{\partial x}$$

where τ is the wall stress and r the coordinate direction normal to the wall.

2.5 Equation of state

Using the assumption made concerning the equation of state the latter is given by:

$$\rho(p,T) = \rho_0 + \left.\frac{\partial \rho}{\partial p}\right|_{T_o} (p - p_0) + \left.\frac{\partial \rho}{\partial T}\right|_{p_o} (T - T_0)$$

Omitting the temperature term due to the assumption of isothermal conditions and defining the bulk modulus β as follows

$$\beta \equiv \rho_0 \cdot \left.\frac{\partial p}{\partial \rho}\right|_{T_o}$$

one can find the differential form of the equation of state.

$$\frac{d\rho}{\rho} = \frac{dp}{\beta}$$

2.6 Evolution equation for the pressure

For an infinitesimally small volume of a pipe it is possible to assume constant cross section A and constant density ρ . Inserting the differential form of the equation of state into the continuity equation one can find a PDE for the pressure in the volume:

$$\frac{\partial p}{\partial t} = \frac{\beta}{\rho}\frac{\partial \rho}{\partial t} = -\frac{\beta}{\rho}\frac{\partial}{\partial x}\left(\frac{\rho \cdot q}{A}\right) = -\frac{\beta}{A}\frac{\partial q}{\partial x}$$

2.7 Evolution equation for the flow

Defining a lumped friction term and rewriting the momentum equation in terms of flow through this infinitesimally small volume one gets a PDE for the flow in the volume:

$$\rho \cdot \frac{dq}{dt} = -A\frac{\partial p}{\partial x} + \frac{\partial F}{\partial x} + A \cdot \rho \cdot g\frac{\partial h}{\partial x}$$

2.8 Friction

The pressure losses due to friction can be divided into minor and major losses. The minor losses occur due to geometric restrictions as e.g. chokes and curvature. The major losses arise due to friction with the walls of the pipe.

For the major losses the friction gradient is given by

$$\frac{\partial F_{major}}{\partial x} = S\tau_w = S \cdot f\frac{1}{4}\frac{\rho}{2}v^2 = S\frac{f}{4}\frac{\rho}{2}\left(\frac{q}{A}\right)^2$$

Here S is the perimeter of the pipe and τ_w the wall shear stress which is related to the Darcy friction factor f as stated. For transition states and turbulent flow the Darcy friction factor can be approximated by the Blasius Theorem as:

$$f = 0.316 \cdot \mathrm{Re}^{-0.25}$$

Here Re is the Reynolds number given by

$$\mathrm{Re} = \frac{\rho \cdot v \cdot d}{\mu},$$

with d as the diameter of the pipe and μ as the viscosity of the fluid.

The friction gradient for the minor losses is dependent on the empirical minor loss gradient $\partial K / \partial x$ as follows:

$$\frac{\partial F_{\min\ or}}{\partial x} = \frac{\partial K}{\partial x} A \frac{\rho}{2} \left(\frac{q}{A} \right)^2$$

The pressure profile in a control volume due to friction and gravity can be gained by integration:

$$p(l) = p(0) - G_f(\rho, \mu, A, q, K) + \rho \cdot g(h(0) - h(l))$$

Defining a G_f as the pressure loss due to friction as follows

$$G_f(\rho, \mu, A, q, K) = (B_0 + f \cdot B_1) \frac{\rho}{2} q^2,$$

with the two constants:

$$B_0 = \int_0^l \frac{\partial K}{\partial x} \frac{1}{A(x)^2} dx$$

$$B_0 = \int_0^l \frac{1}{4} \frac{S(x)}{A(x)^3} dx$$

3 Modelling of the different parts

3.1 The choke

The flow through a valve can be modelled as an orifice flow. For a simple model the following approximations are made:

1) The liquid in the volume of the choke is incompressible.
2) There is no energy loss due to friction or viscous dissipation.
3) The system is in a steady state.
4) The flow is laminar.
5) Contributions due to gravity can be neglected.

Starting from Bernoulli's equation using the assumptions made above it is straight forward to come to an equation of the form:

$$q_c = A_1 A_2 \sqrt{\frac{2(p_c^{in} - p_c^{out})/\rho}{A_1^2 - A_2^2}}$$

Lumping all the constants together into the choke constant K_c and multiplying by a characteristic function $G(z_c)$ describing the opening of the choke one gets the form:

$$q_c = K_c \sqrt{p_c^{in} - p_c^{out}}\, G(z_c)$$

The factor z_c is a controlled variable in the range $0 < z_c < 1$ representing the opening of the choke.

This equation holds for the assumptions made above, but will also be used in the dynamic case. Due to the assumption of an incompressible fluid and no change of energy it is possible to ignore the volume of the choke in a first approximation. This means the inflow and outflow of the choke are equal and denoted as the choke flow.

3.2 The ESP

The pressure increase provided by an electrical submersible pump (ESP) depends on the environmental conditions, e.g. the flow rate and input and output pressure, in addition to the frequency of the pump.

While treating the effect of the pump it is convenient to change from pressure units to head units since in multiphase flows the head is constant for each phase and the Δp varies depending on the density. Therefore most data for the pumps are given in head which is defined as:

$$H = \frac{\Delta p}{\rho \cdot g}$$

In the most basic approach the following assumptions can be made:

6) The energy consumption of the pump is completely neglected.
7) Frictional losses of the fluid inside the pump are compensated by the pump and therefore negligible.
8) Within the pump the fluid is considered to be incompressible.
9) Contributions due to gravity can be neglected.
10) The only input considered is the alternating current of frequency f .
11) The difference between AC-frequency and the rotation frequency of the pump (slip) is neglected.
12) Changes of input parameters are affecting the output of the pump instantaneously.
13) The ESP characteristics for steady state can also be used in the dynamic case.

Each pump has head-flow-characteristics. For a given frequency and water cut, this characteristic gives the relationship between the pump flow and the provided head. This relationship can be used in both directions, i.e. $\Delta p_p(f, q_p)$ or $q_p(f, \Delta p_p)$.

According to the assumptions stated, the ESP is modelled as an instantaneous increase in pressure. This means that at the position of the pump the pressure is described by two values:

$$p_p^{out} = p_p^{in} + \Delta p_p(f, q) \tag{0.1}$$

Assuming no volume means that inflow and outflow are equal so that the flow will be denoted as the ESP-flow.

As stated above, the relationship between increase in pressure and flow through the ESP depends on the mechanical frequency f . The dependency of the characteristics on the frequency is stated by the empirical affinity laws

$$q_2 = q_1 \cdot \left(\frac{f_2}{f_1} \right), \; H_2 = H_1 \cdot \left(\frac{f_2}{f_1} \right)^2 .$$

For an illustration of the affinity laws and ESP characteristics, see Figure 2.

From these two equations, one can from the characteristics of one frequency get the characteristics for all frequencies. There are in reality two different frequencies that describe the ESP; the electrical AC frequency, and the mechanical frequency. In our simple model of the ESP, we set the mechanical frequency equal to the AC frequency, but this is in reality not correct (see assumptions). In addition to the slip, the AC frequency changes are approximately instantaneous, but the mechanical frequency changes are slower. To improve this we use a second order filter to get smooth transitions in the ESP frequency. This is described in more detail in the section on control.

The ESP characteristics are usually given as a polynomial with coefficients a_i for a given reference frequency, and the polynomial for different frequencies is given by the affinity laws. However, the ESP characteristics also depend on the water cut wc . To include this, we calculated for the reference frequency the dependence of the coefficients a_i on the water cut. This is illustrated in Figure 3.

We used the data from the ESP "HC20000 64 stg. – 1100HP", but it is straight forward to include other ESP characteristics. How this is done is described in the appendix section.

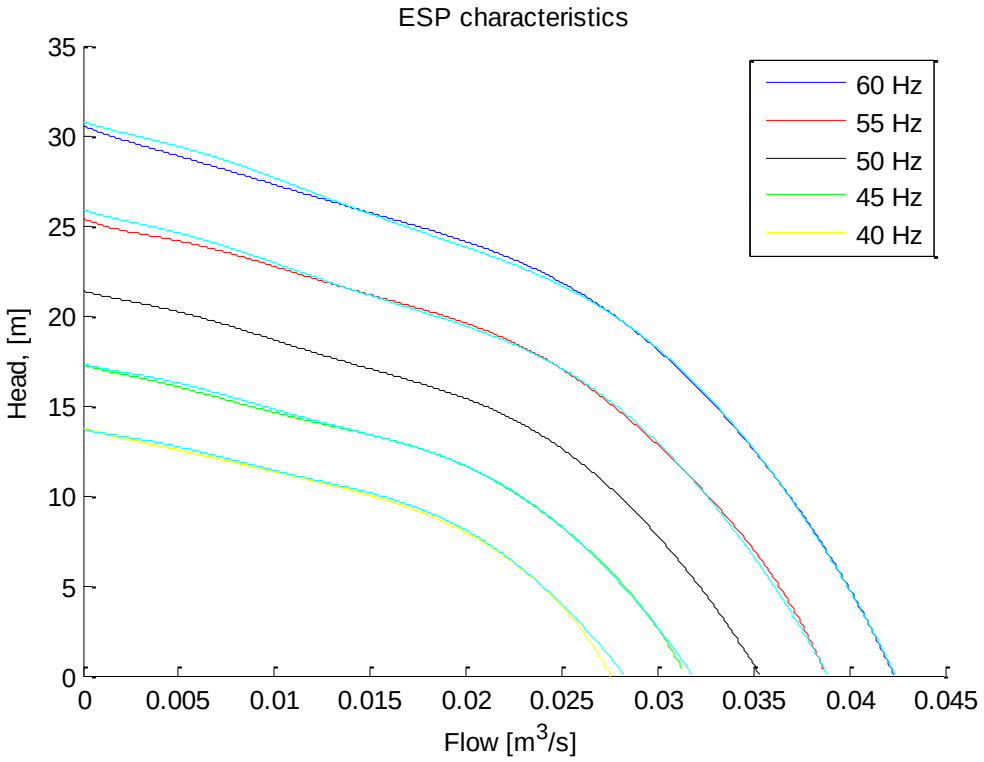

Figure 2: This figure shows what the ESP characteristics look like for different frequencies. The cyan lines are the lines produced by applying the affinity laws to the 50 Hz ESP characteristic line.

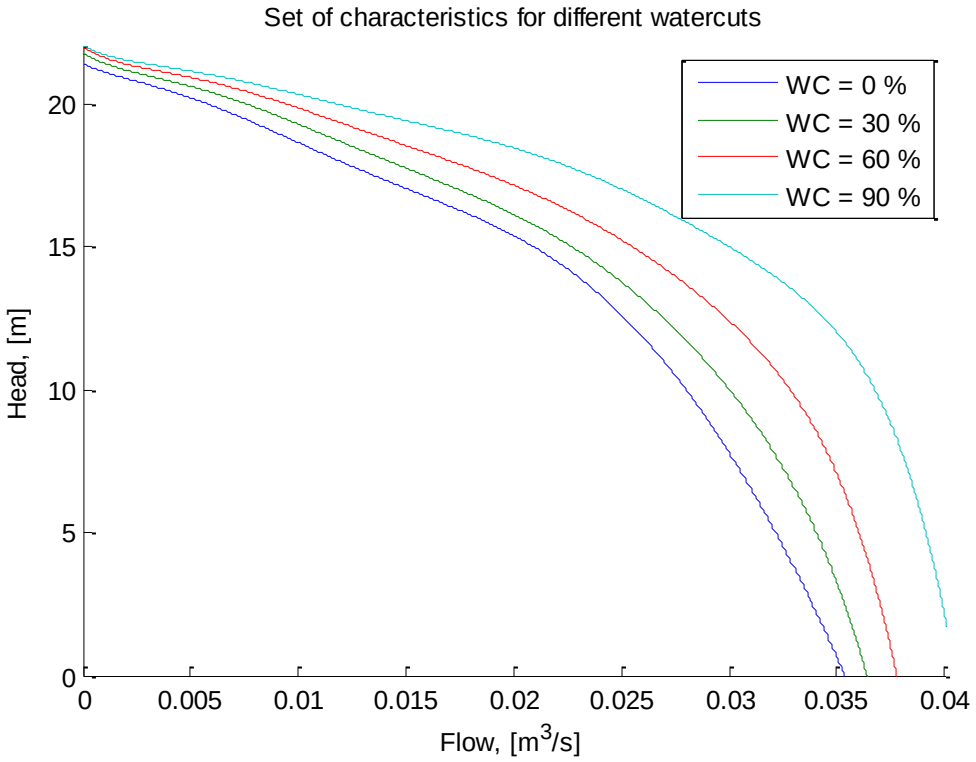

Figure 3: This figure illustrates the ESP characteristics for different water cuts. Data was provided for water cuts of 0 %, 40 % and 90 %. The ESP characteristics for other water cuts are calculated by calculating the coefficients a_i for the reference frequency at different water cuts. The coefficients are then fitted by a second degree polynomial to get dependent $a_i(wc)$.

3.3 The reservoir

One way to model a reservoir is to treat it as a cylindrical surface of the well consisting of a sandface which is permeable. The simplest approach to descirbe the inflow performance of oil wells is the use of the productivity index (PI) concept. The following assumptions are made:

14) The flow is radial around the well.

15) The liquid is incompressible and consists of just a single phase.

16) The permeability distribution of the formation is homogeneous.

17) The formation is fully saturated with the given liquid.

18) The flow and pressure distribution is in a steady state.

With these assumptions Darcy's equation can be applied

$$q = \frac{-\kappa A}{\mu}\frac{(p_{in} - p_{out})}{L},$$

where A is the cross-sectional area of the well, μ the dynamic viscosity of the fluid and L is the length and κ the permeability of the sand face.

Lumping all the reservoir specific constants together into the productivity index the model states a linear inflow performance relation (IPR) which is given by:
$q_r = PI\,(p_r - p_{FBHP})$

Here p_r is the pressure in the reservoir, q_r the flow out of the reservoir and p_{FBHP} the pressure inside the well (Flow Bottom Hole Pressure). The constant PI changes within the lifespan of a well, but can be treated as a constant small time intervals.

Since this model just describes the sand face of the well it does not consist of any volume and therefore no in- or outflow but only the flow though the surface. This will be denoted as the reservoir flow.

Though a steady state is assumed, this model will be used in the dynamic case as well.

4 The one well model

In the one well model we solve the equations derived above numerically with given boundary conditions. We choose to use the reservoir pressure p_r and the downstream choke pressure p_c^{out} as boundary conditions because this will make generalization to N interacting wells easier. We first present a very simple model, and then present a more accurate model afterwards.

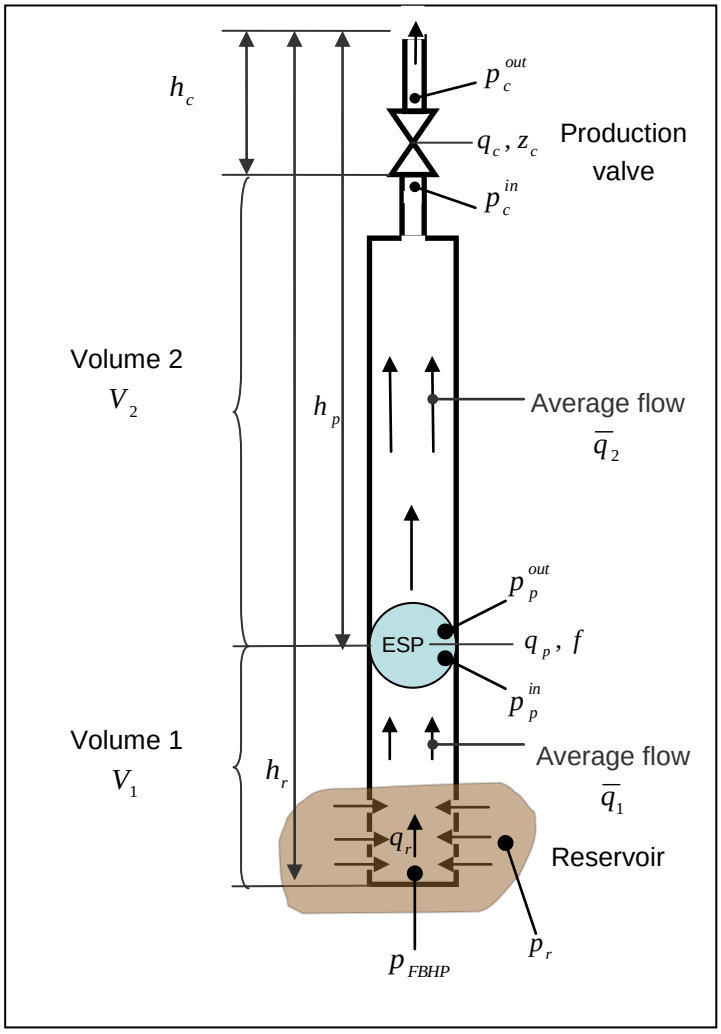

4.1 The simple model

The most simple model in this approach is to only have one control volume for the pressure on each side of the ESP when modelling the pipes. A document on this model was written by Alexey Pavlov, and the main parts are presented here.

4.1.1 Parameters and variables

In this model the well is divided into two volumes, a upstream volume V_1 and a downstream volume V_2 (the terms upstream and downstream are understood here with respect to the ESP). The corresponding bulk moduli of the liquid inside each volume are denoted by β_1 and β_2, respectively, while the densities of the liquid in these volumes are denoted by ρ_1 and ρ_2. This means that the fluids in the two tubing sections can have different fluid properties, witch may be because of a gas separator located below the ESP. The true vertical depth of the pump is denoted by h_p, while the true vertical depth of the bottom is denoted by h_r. It is assumed that h_p and h_r are measured with respect to the position of pressure sensors: Upstream choke-ESP and upstream choke-bottom hole. It is also assumed that the vertical distance between upstream and downstream sensors at the ESP can be neglected.

The following variables are used in the model (see the figure above): reservoir pressure p_r, flow bottom hole pressure p_{FBHP}, pump inlet and outlet pressures p_p^{in}, p_p^{out}, choke inlet and outlet pressure p_c^{in}, p_c^{out}, reservoir flow q_r, pump flow q_p, choke flow q_c. The average flows in the volumes are denoted $\overline{q}_1$, $\overline{q}_2$ and for the whole well $\overline{q}$.

4.1.2 The average pressure and flow model

For modelling the pressure, the PDE derived in the theory is used:

$$\frac{\partial p}{\partial t} = -\frac{\beta}{A}\frac{\partial q}{\partial x}$$

Additionally the following assumption is made:

- The change with respect to time in average pressure is the same as the change in pressure anywhere in the control volume:

$$\dot{\overline{p}} = \frac{\partial p}{\partial t}$$

Considering a control volume of length L and volume $V = A \cdot L$ the PDE then simplifies to:

$$\dot{p} = \frac{\beta}{A \cdot L}(q^{in} - q^{out}) = \frac{\beta}{V}(q^{in} - q^{out})$$

The flow is modelled in the way presented in the theory part, with the equation

$$\rho \cdot \frac{dq}{dt} = -A\frac{\partial p}{\partial x} + \frac{\partial F}{\partial x} + A \cdot \rho \cdot g \frac{\partial h}{\partial x}$$

Additionally the following assumption is made:

- The average flows in the two volumes coincide and are equal the pump and average flow in the whole system:

$$\overline{q}_1 = \overline{q}_2 = q_p = \overline{q}$$

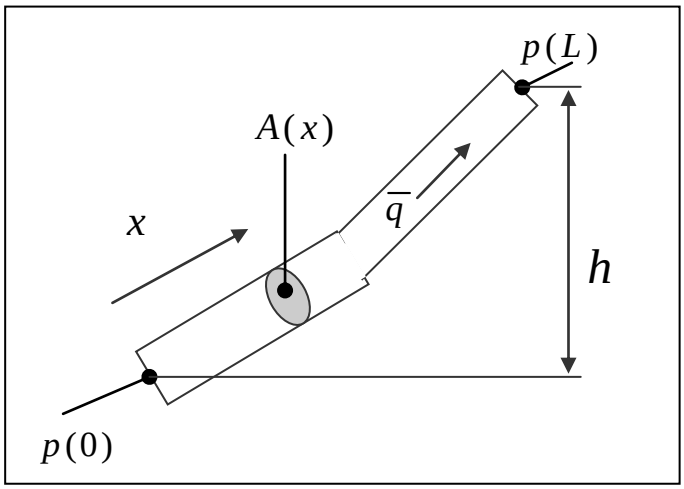

Considering the whole system, the ODE for the flow then is given by:

$$M\dot{\overline{q}} = p^{in} - p^{out} + \Delta p_p - \Delta p_g - G_f$$

where $\overline{q}$ is the average flow, Δp_p is the pressure difference provided by the ESP, Δp_g the hydrostatical term and G_f the pressure loss due to friction. The fluid inertia parameter M is calculated according to the formula

$$M = \bar{\rho} \int_0^L \frac{1}{A(x)} dx$$

Where L is the length of the volume and $A(x)$ the cross-section area of the volume at point x .

4.1.3 *Combining the models of the different parts*

Inserting the reservoir model in the differential equation for the first volume it is possible to derive an equation for the flow bottom hole pressure p_{FBHP} :

$$\dot{p}_{FBHP} = \frac{\beta_1}{V_1}(q_r - \bar{q}) = \frac{\beta_1}{V_1}\left[PI\,(p_r - p_{FBHP}) - \bar{q}\right]$$

By applying the choke model to the differential equation for the second volume one gets an equation for the choke pressure:

$$\dot{p}_c^{in} = \frac{\beta_2}{V_2}(\bar{q} - q_c) = \frac{\beta_2}{V_2}\left[\bar{q} - K_c \cdot G(z_c)\sqrt{p_c^{in} - p_c^{out}}\right]$$

Inserting the friction- and ESP-model the differential equation for the average flow reads:

$$\dot{\bar{q}} = \frac{1}{M}\left[p_{FBHP} - p_c^{in} + \Delta p_p - \rho_1 \cdot g \cdot (h_r - h_p) - \rho_2 \cdot g \cdot (h_p - h_c) - G_{f1} - G_{f2}\right]$$

Here $\Delta p_p(f, q, WC)$ is the pressure difference provided by the ESP, G_{f1} and G_{f2} the pressure losses due to friction in the pipes.

4.2 The complex model

In the simple model we only used one control volume for pressure on each side of the ESP, and only one flow. In order to solve the equations for $\dot{p}$ and $\dot{q}$ more accurately, we need to divide the system in to more control volumes. We here divide the whole length of the tubing into control volumes with constant length.

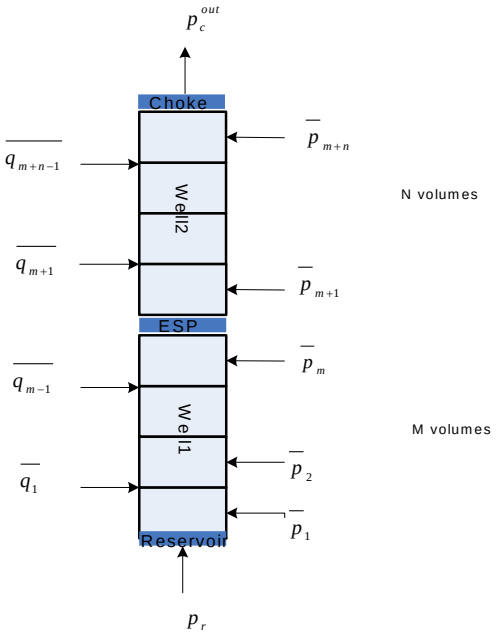

4.2.1 *Parameters and variables*

As stated above, the tubing is now divided into several control volumes, that is m control volumes between the reservoir and the ESP, and n control volumes between the ESP and the choke as illustrated in the figure above. A staggered grid is used, so it is important to remember that the pressures and the flows are not defined at the same points. The pressures and the flows in all the control volumes is denoted by $p_1, \ldots, p_{m+n}$ and $q_1, \ldots, q_{m+n-2}$.

We assume a constant bulk modulus in each pipe, β_1 between the reservoir and the ESP, and β_2 between the ESP and the choke. We also use two different densities in the momentum equation, ρ_1 between the reservoir and the ESP, and ρ_2 between the ESP and the choke, and correspondingly two different viscosities μ_1 and μ_2.

The height of the reservoir is denoted by h_r, the height of the ESP by h_p, and the height of the choke by h_c. The function $h(l)$, read as height as a function of length, is provided by the well geometry, and is needed to compute the friction and hydrostatical terms.

4.2.2 *The average pressure and flow model*

The averaging of the continuity equation in the complex model is done in the same way as for the simple model, so the derivation will not be repeated here. The resulting equation is

$$\dot{p} = \frac{\beta}{V}(q^{in} - q^{out})$$

The averaging of the momentum equations is also done in the same way, but the flows in all the control volumes is now in general not equal. We therefore get

$$\frac{\rho \cdot l}{\overline{A}}\dot{q} = p_{in} - p_{out} - \Delta p_g - G_f ,$$

where Δp_g is the hydrostatical pressure drop, and G_f the pressure loss due to friction.

By introducing the discretization stated above with m and n control volumes, one can write the equations above in a way that makes the implementation on a computer seem more natural. The continuity equation then takes the form

$$\frac{V_i}{\beta_{t1}}\frac{dp_i}{dt} = q_{i-1} - q_i$$

for the control volumes between the reservoir and the ESP. The momentum equation for the flows is by the same notation

$$\frac{\rho_1 l_1}{\overline{A}_i}\frac{dq_i}{dt} = p_i - p_{i+1} - \left[B_{0,i} + f_1 \cdot B_{1,i}\right]\frac{\rho_1}{2}q_i^2 - \rho_1 g\left[h_i^{stg} - h_{i+1}^{stg}\right],$$

where our friction model is inserted. f_i denotes Darcy's friction factor in control volume i. The index i denotes number of the control volume. The superscript stg denotes that the quantity is defined at pressure grid points (the staggered grid), and quantities without it is defined at flow grid points. The constants $\overline{A}_i$, $B_{0,i}$, $B_{1,i}$ and h_i^{stg} have to be calculated from the well geometry by the formulas given previously in the theory section. The corresponding equations for the pipe between the ESP and the choke are given by replacing the constants β_1 etc. by the ones describing the fluid between the ESP and the choke.

4.2.3 Combining the models of different parts

We see from the four previous equations that we encounter problems at the boundaries between different parts of the well. For example in the very first equation, what is q_0? Let's start at the reservoir and proceed upwards. We need an equation for $\dot{p}_1$ that doesn't include q_0. This can be done by replacing q_0 by q_r, but a way to calculate the reservoir flow is needed. Using that the p_1 grid point is separated from one half of a control volume from the bottom hole, we get the relation

$$p_{FBHP} = p_1 + \left[B_{0,1}^{stg} + f \cdot B_{1,1}^{stg}\right]\frac{\rho_1}{4}q_1^2 + \rho_1 g\left[h_r - h_1^{stg}\right].$$

The flow bottom hole pressure is related to the reservoir flow by the equation

$$q_r = PI\,(p_r - p_{FBHP}),$$

and by using these two equations to replace the reservoir flow in the equation for $\dot{p}_1$ we get

$$\frac{V_1}{\beta_1}\frac{dp_1}{dt} = PI\left(p_r - p_1 + \left[B_{0,1}^{stg} + f_1 \cdot B_{1,1}^{stg}\right]\frac{\rho_1}{4}q_1^2 + \rho_1 g\left[h_r - h_1^{stg}\right]\right) - q_1.$$

The same kind of problem occurs at the ESP, and we therefore need a special equation for $\dot{p}_m$ and $\dot{p}_{m+1}$ as well. Here the problem is that the flow q_m, is not defined in the usual way, but is the flow through the ESP, q_p given by the ESP characteristics $q_p = q_p(\Delta p_p, f, wc)$. To calculate this flow by using the ESP characteristics, we need the increase in pressure from the ESP. Since p_m and p_{m+1} is defined in a staggered grid, the pressure increase from the pump is not given by $\Delta p_p \neq p_{m+1} - p_m$. We have to take into account the pipe sections between the pressure grid points and the ESP. We then get the following equations for the pump input and output pressure:

$$p_p^{in} = p_m - \left[B_{0,m}^{stg} + f_{m-1} \cdot B_{1,m}^{stg}\right]\frac{\rho_1}{4}q_{m-1}^2 - \rho_1 g\left[h_m^{stg} - h_p\right],$$

$$p_p^{out} = p_{m+1} + \left[B_{0,m+1}^{stg} + f_{m+1} \cdot B_{1,m+1}^{stg}\right]\frac{\rho_2}{4}q_{m+1}^2 + \rho_1 g\left[h_p - h_{m+1}^{stg}\right],$$

and the pressure increase from the ESP is now given by $\Delta p_p = p_p^{out} - p_p^{in}$. And the equation for $\dot{p}_m$ and $\dot{p}_{m+1}$ is then given by

$$\frac{V_m}{\beta_1}\frac{dp_m}{dt} = q_{m-1} - q_p(\Delta p_p, f, wc),$$

$$\frac{V_{m+1}}{\beta_1}\frac{dp_m}{dt} = q_p(\Delta p_p, f, wc) - q_{m+1}.$$

The last problem of this type occurs at the last pressure control volume before the choke. There the flow q_{m+n-1} is not defined and should be replaced by q_c given by the choke equation

$$q_c = K_c\sqrt{p_c^{in} - p_c^{out}}\,G(z_c),$$

where p_c^{out} is given by the boundary conditions. p_c^{in} on the other hand has to be calculated in the same way the upstream pump pressure was calculated:

$$p_c^{in} = p_{m+n} - \left[B_{0,m+n}^{stg} + f_{m+n-1} \cdot B_{1,m+n}^{stg}\right]\frac{\rho_2}{4} q_{m+n-2}^2 - \rho_2 g\left[h_{m+n}^{stg} - h_c\right].$$

It is noteworthy that because of these bordering pressures, the friction constants B_0 and B_1 have to be calculated also for the staggered grid (the pressure control volumes), and not only for the non staggered grid (the flow control volumes). This is, however, not a very serious complication.

The calculation of $\dot{q}_i$ is straight forward according to the equations given above.

To calculate these bordering pressures, flows from the neighbouring grid points were used. It may seem a little strange to use the flow q_{m-1} as the flow in the region between the grid points of p_m and the ESP. This is on the other hand the closest flow available. The reason we needed to do this special analysis of the bordering pressures, was that without it, that is, using $p_{FBHP} = p_1$, $p_p^{in} = p_m$, $p_p^{out} = p_{m+1}$ and $p_c^{in} = p_{m+n}$, the steady states of our models was considerably different for the simple and the complex model. In addition, the steady states of the complex model would have been highly dependent on the chosen number of control volumes. This special treatment of bordering pressures is therefore necessary.

There is, however, another problem that surface with this approach and causes small deviations in the steady states of the simple model and the complex model with different m and n. This is explained below.

4.3 Steady states

4.3.1 Calculating the steady states

These coupled ordinary differential equations (for both models) have a stationary solution, that is, there exists a steady state where no changes occur in time. These states are also unique for a given set of parameters. To get this steady states, all time derivatives is set equal to zero, and the resulting equations gives the steady state solution to the original time dependent equations.

By looking at the continuity equation, one can easily see that setting $\dot{p} = 0$ results in constant flow, $\partial q / \partial x = 0$. By also setting $\dot{q} = 0$, one gets from the simple model

$$p_c^{in} = p_{FBHP} + \Delta p_p - \rho_1 \cdot g \cdot (h_r - h_p) - \rho_2 \cdot g \cdot (h_p - h_c) - G_{f,1} - G_{f,2},$$

which states that the total pressure loss in the well is the pressure loss due to friction, plus the hydrostatical pressure loss, minus the pressure increase from the pump. The pressure drops due to friction, $G_{f,1}(q)$ between the reservoir and the ESP, and $G_{f,2}(q)$ between the ESP and the choke need to be calculated. From the complex model we get the following equation

$$p_{i+1} = p_i - \left[B_{0,i} + f_i \cdot B_{1,i}\right]\frac{\rho_{t1}}{2} q^2 - \rho_{t1} g \left[h_i^{stg} - h_{i+1}^{stg}\right],$$

which states that the pressure loss in one control volume is the sum of the pressure loss due to friction and the hydrostatical pressure loss. By remembering that the whole piping is taken into account by the formulas for the bordering pressures given above, one soon realizes that the steady state solution of the two different models should be the same. However, there are small deviations in the steady states that will be discussed later.

We wish to use the steady state as the initial condition for our solution of the differential equations. The steady state flow q and pressure profile $p(l)$ then has to be calculated.

This is done by solving the equation

$$p_{FBHP}(q) - p_c^{in}(q) + \Delta p_p(q) - \rho_1 \cdot g \cdot (h_r - h_p) - \rho_2 \cdot g \cdot (h_p - h_c) - G_{f,1}(q) - G_{f,2}(q) = 0,$$

where the flow bottom hole pressure is related to the reservoir pressure and flow by the PI equation, and the upstream choke pressure is given by the choke equation.

The equation should be solved with respect to the flow q. This is very complicated, maybe impossible, because the complicated relation $\Delta p_p(q)$ from the ESP characteristics and (possible) complicated well geometry. Therefore this equation is solved numerically. How this is done is described in the section on implementation.

4.3.2 Analyzing the steady states

There are small deviations in the steady states as seen in *Figure 4* and Figure 5.

The reason for these deviations is the complicated well geometry, and there are two main issues that cause deviations:

- The friction constants $B_{0,i}^{stg}$ and $B_{1,i}^{stg}$ used to calculate the bordering pressures (the flow bottom hole pressure, upstream and downstream ESP pressure, and the upstream choke pressure) are really defined in the whole pressure control interval and not only in the half closest to the border. We therefore used half this value, but when the well geometry is complicated, that is, the well is not linear, this will not be correct. This causes small deviations between the steady states of the complex model with different number of control volumes.

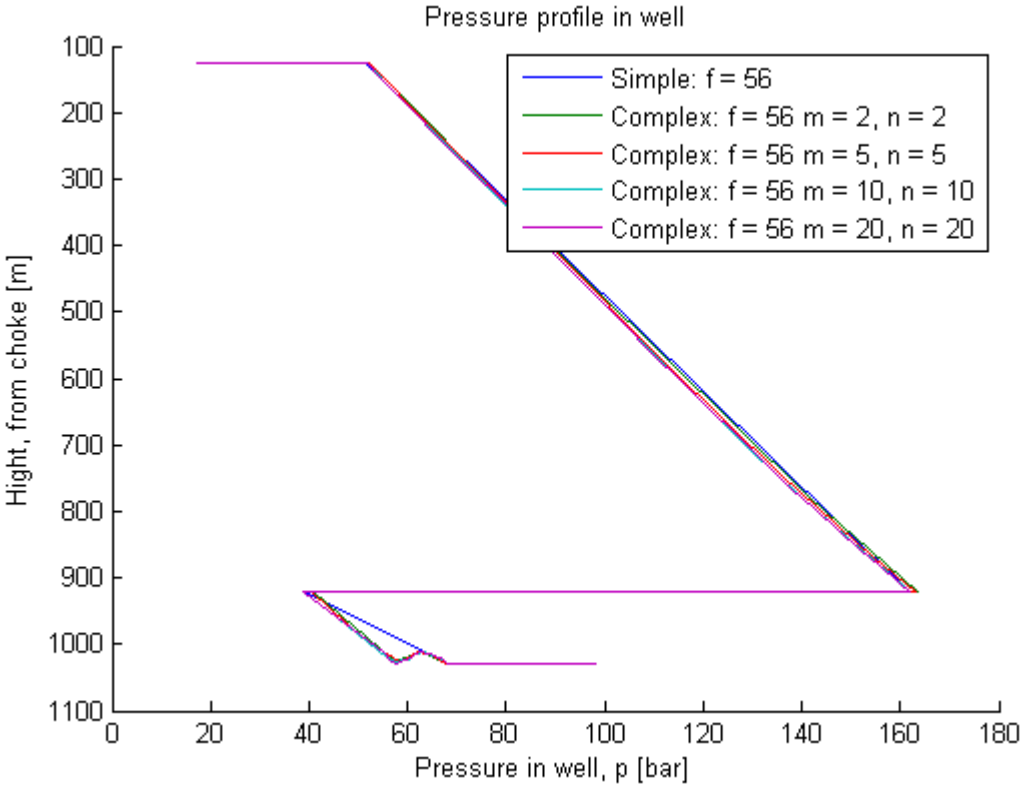

Figure 4: This figure shows the pressure profiles in the well for different models.

- To calculate Reynolds number, a pipe radius is needed. In the simple model the average pipe radius is used, and in the complex model the local radius is used. This causes a small deviation between the steady states of the simple model and the complex model with different number of control volumes.

Both these effects can be seen in *Figure 4* and Figure 5. The first point can be fixed by calculating the specific friction constant for these "half control volumes", but the second point is not that easily corrected. Both effects, however, only cause small deviations that are not really important on the accuracy scale of these models.

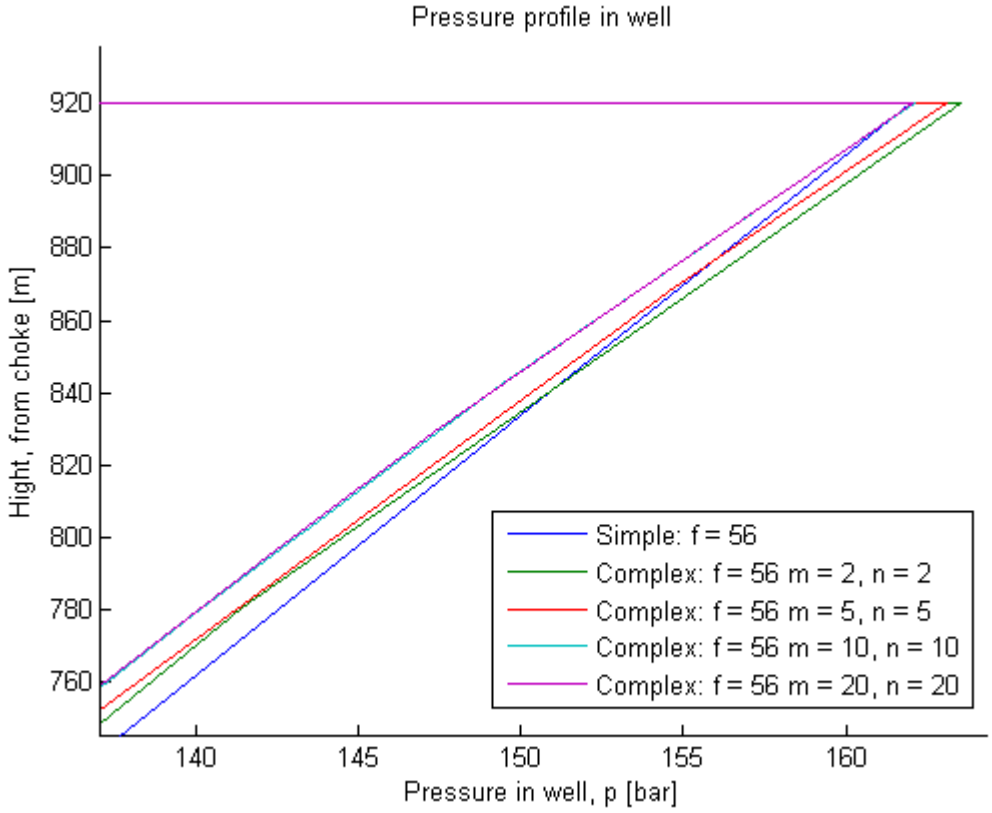

Figure 5: This figure shows the pressure profile calculated by different models with zoom. From this figure it can be seen that the pressure profiles are not identical.

5 N interacting wells

We now wish to model a set of N wells connected to the same manifold as illustrated in the figure below. Because of time limitations, we only had time to implement a very simple model for the production manifold, and in addition using only the simple model for one well described above. However, it should not be difficult to replace the simple model for one well with the complex one.

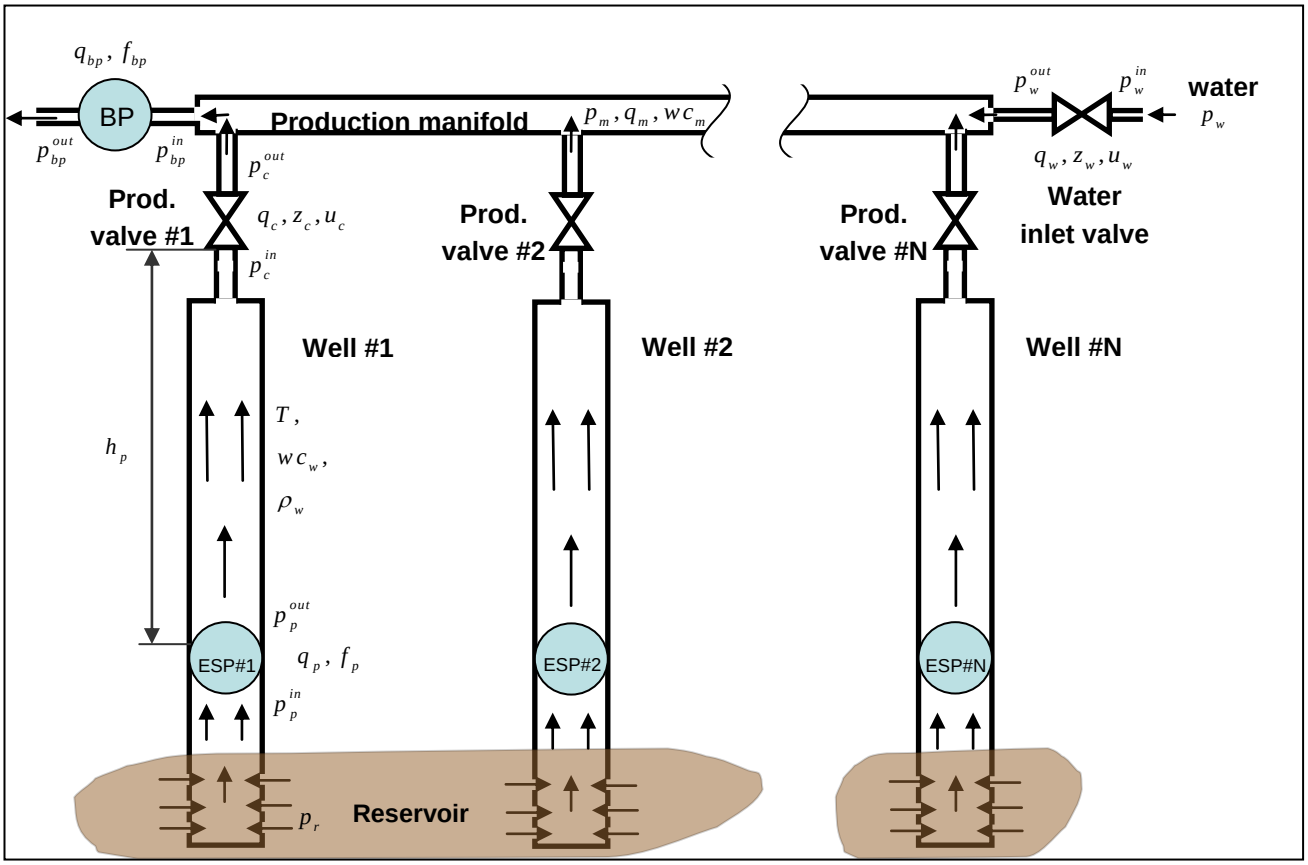

5.1 Simple manifold model

We model the manifold as a horizontal pipe with only one control volume. Each well is connected to this volume, so that the downstream choke pressure of each well will be equal to the manifold pressure, and the flow from one well to the manifold is equal to the choke flow. The only interaction between the wells is therefore at the manifold, where every well has a common downstream choke pressure.

The model of the production manifold also includes a water valve (WV) and a booster pump (BP). The water valve is modelled as a choke with constant K_{WV} with a net inflow of

fluid q_{WV} . The water valve characteristics are now the same as that of the production chokes, but it is easy to implement other characteristics. The booster pump is modelled in three different ways: The first way is to model it as an ESP with a corresponding frequency and characteristic (implemented), the second way is to model it as a pump providing a constant outflow q_{BP} independent on the pressure difference over the booster pump, Δp_{BP} (implemented). The third one is to model it as a pump providing a constant head (not implemented).

The approach to model the booster pump as an ESP will cause problems because of the restricted flow regimes in the ESP characteristics.

As boundary conditions it is now natural to use (depending on the booster pump model) the booster pump output pressure, p_{BP}^{out} (or the booster pump flow), and the input water valve pressure p_{WV}^{in} in addition to the reservoir pressure p_r .

5.1.1 *Dynamic equations for the manifold*

The time evolution of the manifold pressure p_{man} is given by the equation

$$\frac{V_{man}}{\beta_{man}} \frac{dp_{man}}{dt} = q_{man}^{in} - q_{man}^{out} ,$$

where V_{man} is the volume of the manifold piping and β_{man} is the bulk modulus of the fluid in the manifold. The inflow to the manifold is given by the sum of all choke flows q_c^i from all the wells, plus the inflow from the water valve:

$$q_{man}^{in} = q_{WV} + \sum_{i=1}^{N} q_c^i ,$$

while the outflow is given by the booster pump flow, $q_{man}^{out} = q_{BP}$.

For each of the wells, the same equations can be used by replacing the downstream choke pressure in all the wells (here generalized by the index i) by the manifold pressure $p_c^{out,i} = p_{man}$.

5.1.2 *Steady state*

The steady state solution for the N wells equations is of course dependent on the number of wells N , and gets rather complicated. The explicit form of the equations will therefore not be presented here.

From the equation given above for the time evolution for the manifold pressure, one gets that the inflow and the outflow from the manifold is constant in the steady state. If an

analytical solution to the one well steady state problem had been found, that is an expression for the flow, the solution of the N well problem would be given by inserting the formula for the steady state flow q_i for well i into the equation

$$q_{BP} = q_{WV} + \sum_{i=1}^{N} q_i ,$$

and inserting the choke equation for q_{WV} and ESP characteristics for q_{BP} (or just keep q_{BP} depending on preference). The downstream choke pressure in the formula for q_i should be replaced by the manifold pressure p_{man}. This results in an equation on the form $G(p_{man}) = 0$, which in turn could be solved for the manifold pressure. This is, however, even more complicated than for the one well case, and a numerical solution strategy will be outlined below.

If the wells are identical, that is all the ESPs are working at the same frequency with the same characteristics, the choke openings, constants and characteristics are identical, the reservoir pressures are identical and the well geometries are the same, there is nothing in the manifold equation to distinguish one well from another. Therefore, the flows in all the wells should be identical in the steady state. This is a very useful test to do to check the numerical solution method of the steady state equation.

In addition, if all the wells are identical, the wells should react in the same way, meaning that if the ESP frequency is changed in one well, all the other wells should react identically. This is a useful test to do when solving the equations numerically.

6 Implementation and numerical issues

In this section, the implemented approach for solving both the static equations and the dynamic equations will be discussed. Encountered problems with possible solutions will be given. For a detailed description of the different program functions, see the appendix.

6.1 Solving the steady state equation for one well

The equation for the steady state of the one well problem is as stated previously

$$p_{FBHP}(q) - p_c^{in}(q) + \Delta p_p(q) - \rho_1 \cdot g \cdot (h_r - h_p) - \rho_2 \cdot g \cdot (h_p - h_c) - G_{f1}(q) - G_{f2}(q) = 0 .$$

This is an equation of the form $F(q) = 0$, and the MATLAB function `fsolve` is designed to solve this kind of equation. The implementation is straight forward, and the calculation will result in a steady state flow q. The implementation produces an output on the following form:

```
OK. Error: 1.14e-012
```

This output means that a solution was found, and the relative error in the solution is $1.14 \cdot 10^{-12}$. If the relative error is too high, or if a solution was not found, the program will print out a massage with the corresponding error. Keeping an eye on the MATLAB terminal is therefore a good idea when calculating the steady state (both explicitly and when starting the dynamic calculations).

The reason for the discussed deviation in the steady states is now hidden inside the friction terms $G_{f1}(q)$ and $G_{f2}(q)$.

6.1.1 The pressure profile

The pressure profile needs to be calculated in order to initialize the dynamic calculations. It is also interesting to see how the pressure in the well develops as a function of height or length. This is fortunately not that difficult once the steady state flow is known.

The flow bottom hole pressure can be calculated from the PI equation. The pressure at any point in the well between the reservoir and the ESP can then be calculated from the equation

$$p(l) = p_{FBHP} - \left[B_0(l) + f \cdot B_1(l)\right]\frac{\rho_1}{2}q^2 - \rho_1 g\left[h(l) - h_r\right].$$

Here, l is the length from the bottom hole to the desired pressure point. At any point after the ESP, the same formula can be used, but with the pressure increase from the ESP

added. Alternatively, the pressure in the tube between the ESP and the choke can be calculated from the upstream choke pressure.

6.1.2 *The negative pressure problem*

The main problem we encountered when solving the steady state equations is that for some environmental parameters, the pressure can become negative. This is, of course, not physical, and the reason this occurs is that the steady state equation does not always have a valid solution given our assumptions.

The reason for this is that we have assumed that there is a net downstream flow and a pseudo single phase fluid. To achieve a net downstream flow, the downstream choke pressure has to be smaller than the reservoir pressure minus the pressure drop from friction and gravity. If this condition is not satisfied, the physical system would no longer satisfy our assumptions. The steady state is then a water layer in the lower part of the well, an oil level in the middle of the well, and a gas layer at the top.

Therefore, it is important to watch the pressures when experimenting with the boundary conditions and other quantities so that a valid steady state with positive pressures and flows are found.

6.2 Solving the steady state equation for *N* wells

The steady state equation for the N wells problem is as stated above complicated, but we want to solve it in order to be able to initialize the dynamic calculation with a steady state solution. The steady state equation for one well is given by

$$q_{WV} + \sum_{i=1}^{N} q_i - q_{BP} = 0,$$

where q_{BP} is the booster pump flow, q_{WV} is the water valve flow and q_i is the choke flow from well i. This is then an equation of the form $G(p_{man}, \{q_i\}) = 0$.

The problem with this is that we do not have an analytical expression for the choke flows.

We avoid this problem with the following approach: The function $F(q)$ for one well given above can easily be generalized to N wells. The downstream choke pressure must be replaced by the manifold pressure, and different well geometries have to be taken into account. The equation will be solved on a computer by an iterative process, so we always have a guess for the solution. Therefore the function $F_i(q_i)$ for well i can be calculated, and as for the one well case, this function should be zero, that is $F_i(q_i) = 0$. In addition, the above equation relating the water valve flow to the choke flows and booster pump flows must be satisfied, that is $G(p_{man}, \{q_i\}) = 0$.

The steady state for the N wells can therefore be found by solving these $N+1$ equations. This could be done by again using the MATLAB function `fsolve`, by finding the zero point of the function

$$H(p_{man},\{q_i\}) = G(p_{man},\{q_i\}) + \sum_{i=1}^{N} F_i(q_i).$$

As it turns out, `fsolve` doesn't find a solution. Another approach is to find the minimum point of the absolute value of $H(p_{man},\{q_i\})$ in the multi dimensional $\{p_{man},\{q_i\}\}$ space using the MATLAB function `fminsearch`. This solution method works much better, but there are still problems.

This functions calculates a minimum point witch is close to the steady state, but not exactly the steady state. The minimum point of $\left|H(p_{man},\{q_i\})\right|$ that `fminsearch` calculates does not coincide with the zero point of $H(p_{man},\{q_i\})$. This may be caused by the fact that `fminsearch` finds a local minimum and not the global minimum. This may be taken care of by choosing a better initial guess for the steady state solution. Unfortunately we didn't have time to investigate this further.

This problem can be seen when the dynamic calculation is started. The steady state found by `fminsearch` is actually close to the correct one, but because of the deviation there is some dynamics in the beginning before a steady state is reached. A solution to this problem is to run the dynamic calculation until the real steady state is achieved, and then start the real simulation.

Unfortunately we did not have time to look further into this problem. A different approach for finding the steady state of the N wells system may be need.

6.3 Solving the dynamic equations

We now have a set of coupled first order differential equations that we need to solve for both the single well system and for the N wells system. This is done by using the built in MATLAB function `ode4`, which uses the Runge-Kutta method of forth order with fixed time step.

Other ODE solvers were tried out, both variable time step solvers and implicit solvers, as `ode23` and `ode45`. These solvers were not able to solve the differential equations in the correct way, and caused considerable numerical errors. These errors seemed to originate at the ESP. Therefore, the `ode4` solver was used when calculating the results presented in this report.

The ESP characteristics cause some problems when solving the differential equations. The discussion of these problems with our solution follows.

6.3.1 ESP characteristics – sudden frequency changes

When simulating both a one well system and a N wells system, studying the system's reaction to disturbances is an important issue. However, sudden frequency changes in the ESP cause problems.

Assume a one well system in the steady state with the ESP running at a given frequency f_1. The frequency is then suddenly changed to a new frequency f_2. In the first time step after the frequency change, the program will try to calculate the new pump flow $q_p(\Delta p_p, f_2, wc)$ from the ESP characteristics in order to calculate the right hand side of the differential equations for pressure next to the ESP. This means that in the first time step, we will stay on a constant Δp_p in the characteristics, and then calculate the flow corresponding to the ESP characteristics for the new frequency. However, this flow might be negative. Why? Because the intersection between the ESP characteristics and the constant Δp_p line may be on the negative flow axis. This is not physically reasonable.

The reason for this is that the frequency in the ESP characteristics is in reality the mechanical frequency and not the electrical frequency. The electrical frequency can be changed very suddenly, but the mechanical frequency will need time to change. A sudden frequency transition as described above is therefore not physical.

Our solution to this problem is to say that the frequency cannot be changed suddenly, but needs time to get from one frequency to another. A second order filter was used to calculate the transition between two frequencies. However, this in turn caused oscillations in the pump flow because the rate of the frequency change changes with time. This behaviour is studied more closely in the analysis of the transition states. Therefore, a linear transition between two frequencies was implemented as well. An illustration of this issue is shown in Figure 6 and Figure 7. The figures were produced by using the complex model with two control volumes on each side of the ESP for simplicity.

The frequency transition (either linear or with a second order filter) can be selected in the files `*transition.m`. The frequency change was limited to 0.5 Hz in one second. See the control section for more details on the second order filter.

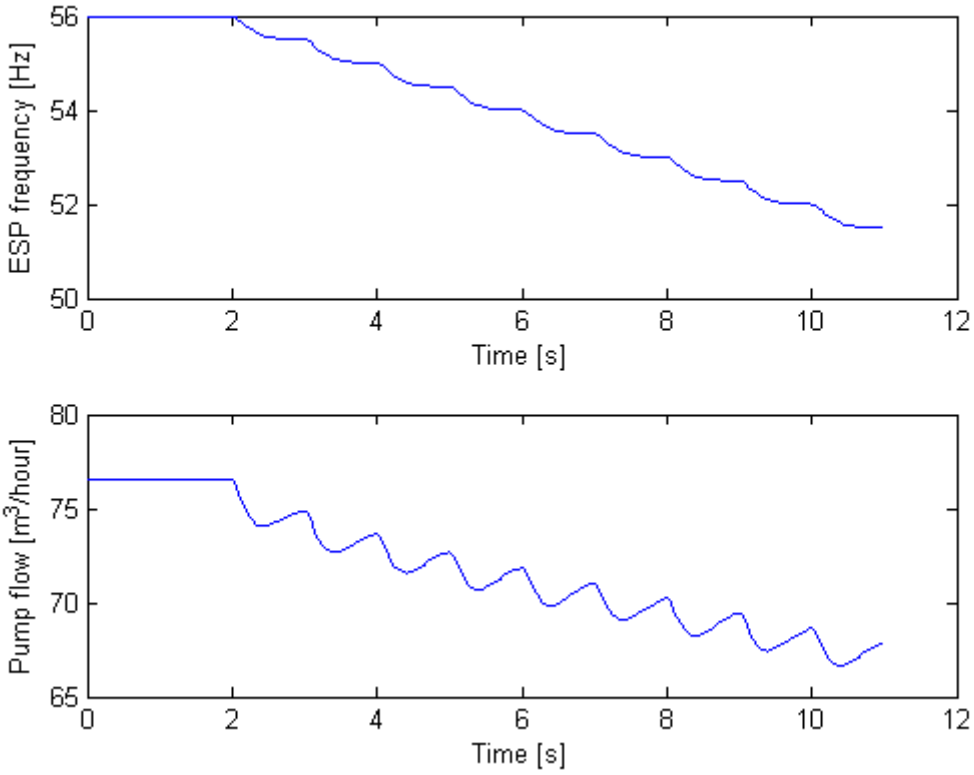

Figure 6: This figure shows the time development of the ESP frequency and pump flow when using a second order filter to make transitions between to frequencies. There are strong oscillations in the pump flow as shown in the lowermost figure.

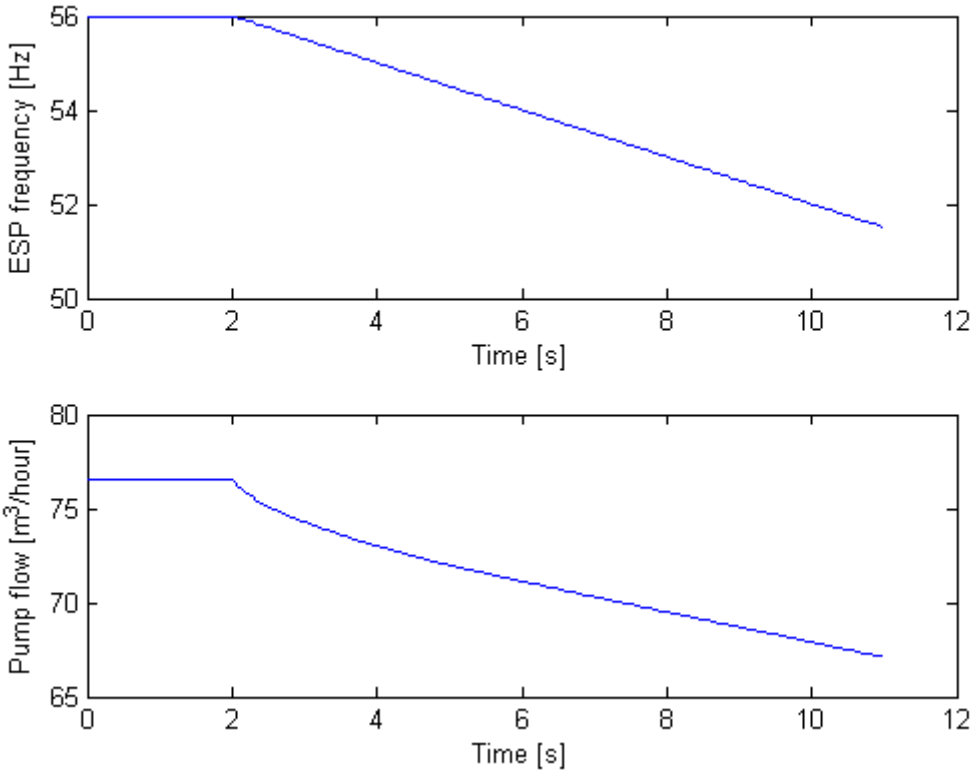

Figure 7: This figure shows the time development of the ESP frequency and the pump flow when using linear frequency transitions. There are no oscillations in the pump flow as can be seen from the lowermost figure.

6.3.2 ESP characteristics – steady states and performance issues

Naturally, we wanted our program to be as fast as possible. The ESP characteristics are usually given by polynomials that express the flow through the ESP as a function of the provided head for a given reference frequency. As can be seen from the differential equations for the complex model, this is exactly what is needed: A function $q_p(\Delta p_p, f, wc)$ that calculates the pump flow from the pressure increase from the ESP and the ESP frequency.

For the simple model and for the steady states, the situation is a little different: A function $\Delta p_p(q_p, f, wc)$ is needed, which is the inverse of the function $q_p(\Delta p_p, f, wc)$. Since $q_p(\Delta p_p, f, wc)$ may be a high order polynomial, finding the inverse will be difficult, maybe impossible. In MATLAB this problem can easily be solved by using the interpolation function `interp1`. By using a high resolution in head and using linear interpolation, Δp_p can be found from a given pump flow q_p.

In terms of performance, this is not a good solution. The interpolation function in MATLAB is very slow, so the use of an interpolation function will cause the program to slow down considerably. This problem can be solved by fitting a polynomial to the function $\Delta p_p(q_p, f, wc)$ as well. This is illustrated in Figure 9.

This is, however, not a perfect solution. The inverse of a polynomial is, of course, not a polynomial, so the fitting will not be perfect. The ESP characteristics calculated from the fitted polynomial will not be the same as those calculated for the original polynomial. This has two consequences: Firstly, since the simple and the dynamic model use different ESP characteristics functions, this will cause new deviations between the two models. Secondly, the steady state solution uses the fitted polynomial and the complex dynamic model's dynamic calculation uses the original polynomial. Therefore, there will be deviations between the calculated steady state and the steady state reached in a dynamic calculation for the complex dynamic model. This can be seen in

Figure 8.

This deviation could have been reduced by increasing the degree of the polynomial for $\Delta p_p(q_p, f, wc)$, we saw that this was not really a good solution either. The deviation in the steady states becomes smaller, but the oscillations shown

Figure 8 increase, and additionally the evaluation of the polynomials becomes slow.

The same problem will, of course, exist if the polynomial is used for $q_p(\Delta p_p, f, wc)$ and interpolation used for $\Delta p_p(q_p, f, wc)$. However, depending on the chosen resolution in head in the interpolation, the deviation can be made very small. The problem can be avoided completely by using in stead of polynomial a set of data points and do interpolation for both $q_p(\Delta p_p, f, wc)$ and $\Delta p_p(q_p, f, wc)$.

Another effect is seen in

Figure 8. The pump flow keeps oscillating around the steady state flow. This is actually because of numerical problems when calculating $q_p(\Delta p_p, f, wc)$ from the polynomial.

The only way to avoid this is to use interpolation in the function $q_p(\Delta p_p, f, wc)$ as well as in the $\Delta p_p(q_p, f, wc)$ function. Alternatively a low degree polynomial could be used, but this in turn results in large deviations between the steady states.

However, the calculation with interpolation is faster than real time. This means that, as long as a very high speed isn't needed, the interpolation method should be used for both functions. All of the described methods are implemented, and which one to use can be chosen in the `dpESP.m` and `qESP.m` functions in the "Modules" folder by commenting in/out the desired

method.

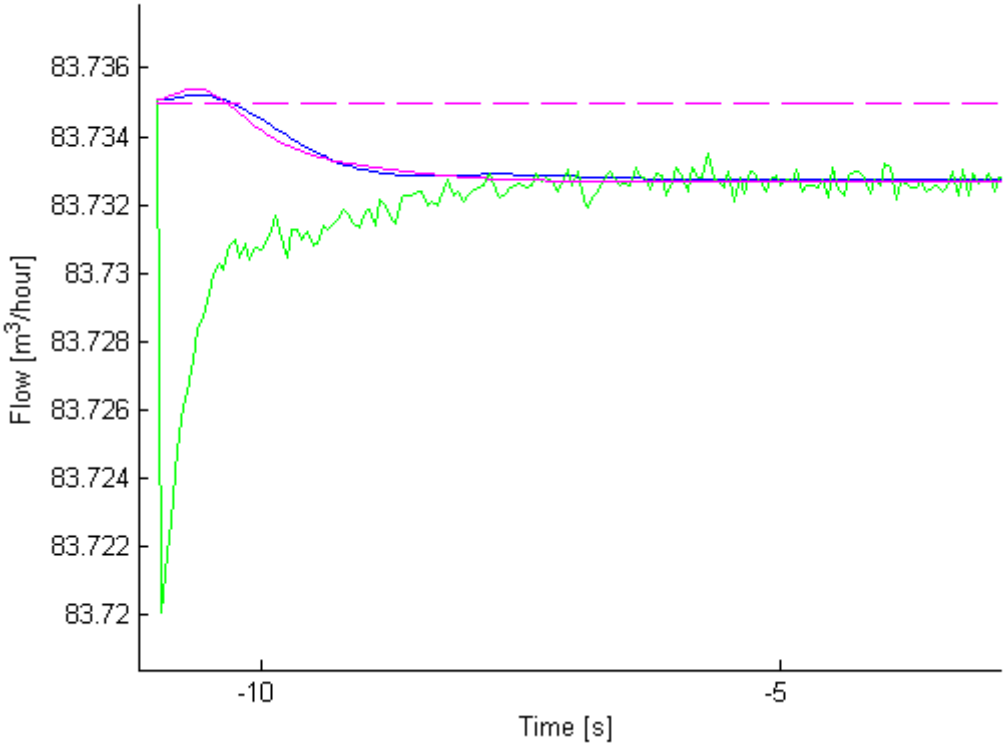

Figure 8: This figure illustrates the deviation in the steady states when a fitted polynomial is used for the inverse function $\Delta p_p(q_p, f, wc)$ *in the calculations. The system is started out in the calculated steady state. Blue is reservoir flow, green is pump flow and magenta is choke flow. The continuous line is the complex dynamic model with two control volumes on each side of the ESP, and the dashed line is the simple model.*

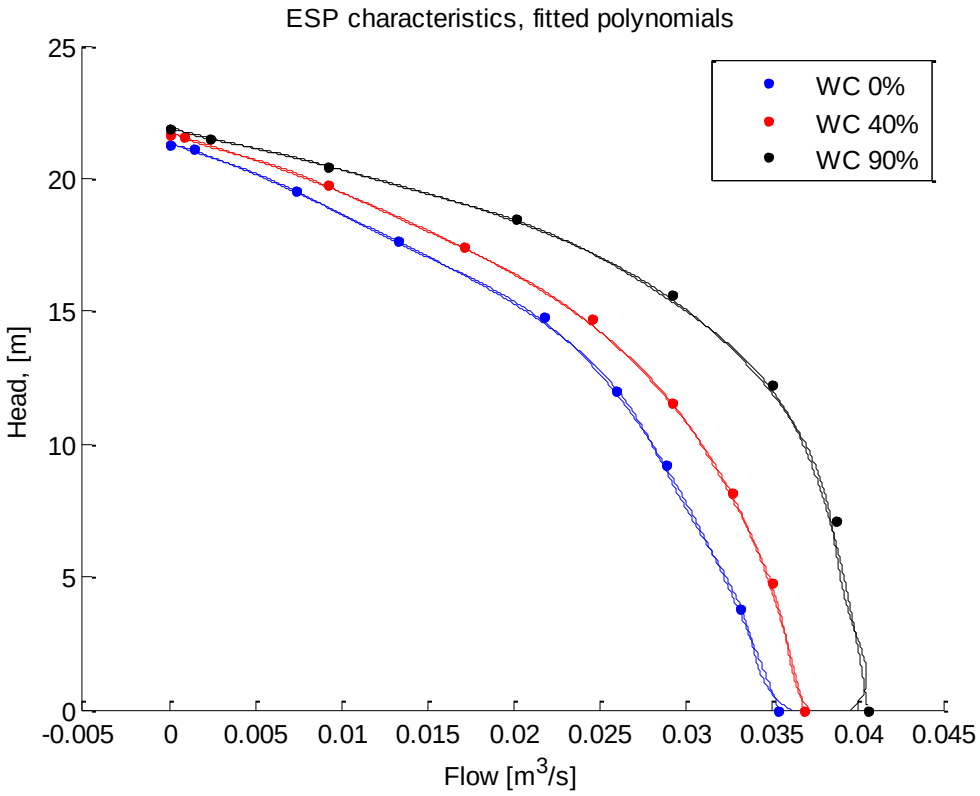

Figure 9: This figure illustrates the fact that polynomials fitted to the data to get both $q_p(\Delta p_p, f, wc)$ *and* $\Delta p_p(q_p, f, wc)$ *do not coincide. Here polynomials of degree seven are used.*

6.3.3 Stability criterion

We are solving a set of coupled ordinary differential equations, but that is because the spatial dimension was discretisized when the averaging of the partial differential equations describing the piping was done. What we are really doing is solving partial differential equations explicitly in time.

This means that there exists a stability criterion that has to be satisfied for the solution method to provide good results. A stability criterion is a relation between the special step length, Δx_1 and Δx_2 in the piping before and after the ESP respectively, and the time step Δt.

Finding such a relation is not within the scope of this project, and it is not necessary in order to get good results. The main thing to remember is that for a chosen number of control volumes, there is an upper limit of the time step Δt that can be used. If the time step is chosen above this limit, the program will crash. The solution is then to decrease

the time step used in the calculations. The general behaviour is that if the number of control volumes is increased, the time step must be decreased.

It is important to investigate the behaviour of the calculated solution as a function of the integration time step Δt to make sure that the solution has converged. This is done in

Figure 10 to Figure 12. A sudden drop in the manifold pressure (downstream choke pressure) was used in order to investigate the solution's dependence on the time step.

From these figures, one clearly sees that a time step of 0.05 seconds captures the dynamics of the system. However, this time step may need to be increased in order to satisfy the stability criterion when the number of control volumes is increased. In the figures presented here, 10 control volumes on each side of the ESP were used.

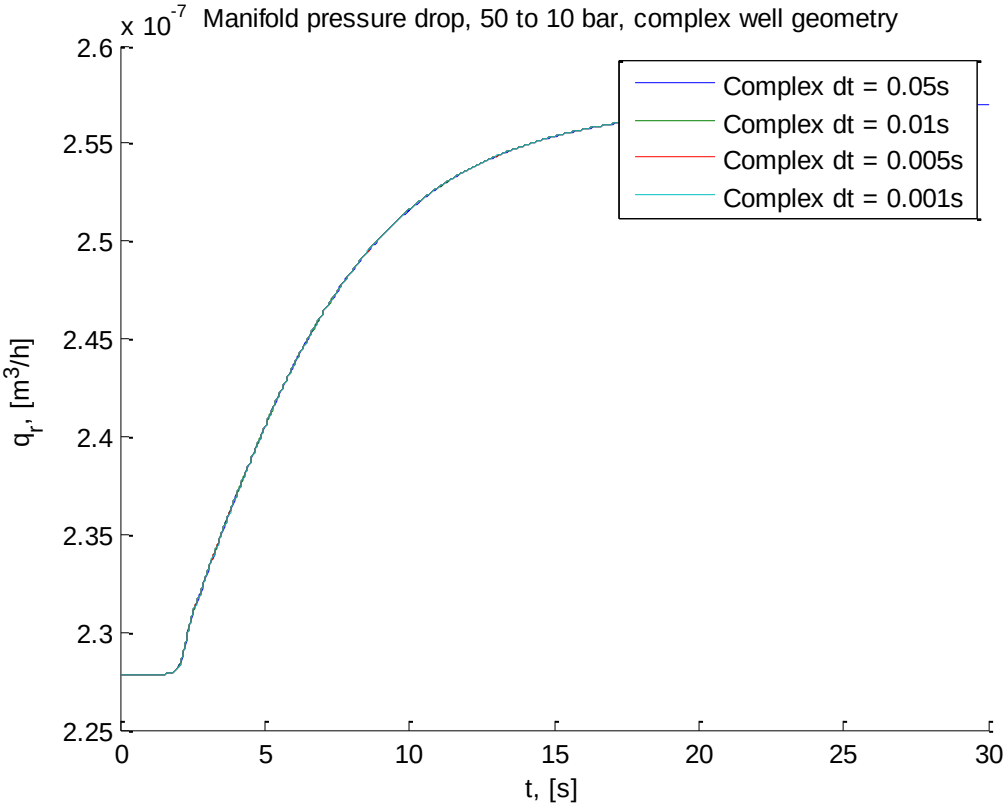

Figure 10: This figure shows the time development of the reservoir flow after a sudden decrease in the manifold pressure for different time steps.

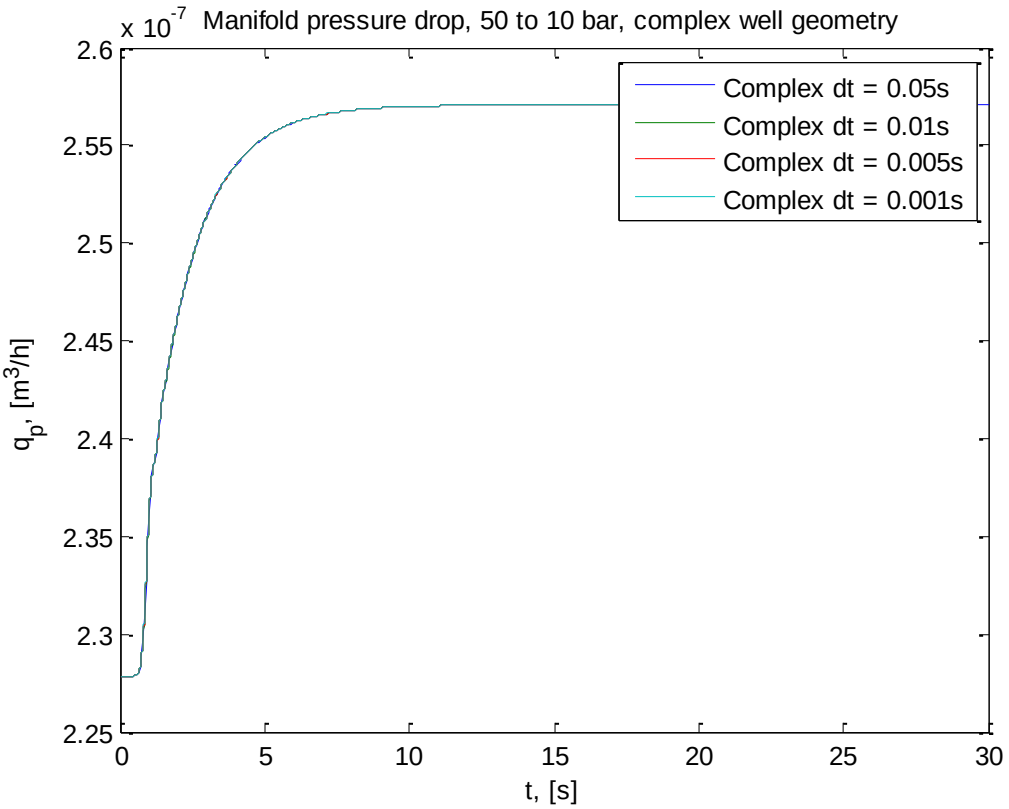

Figure 11: This figure shows the time development of the pump flow after a sudden decrease in the manifold pressure for different time steps.

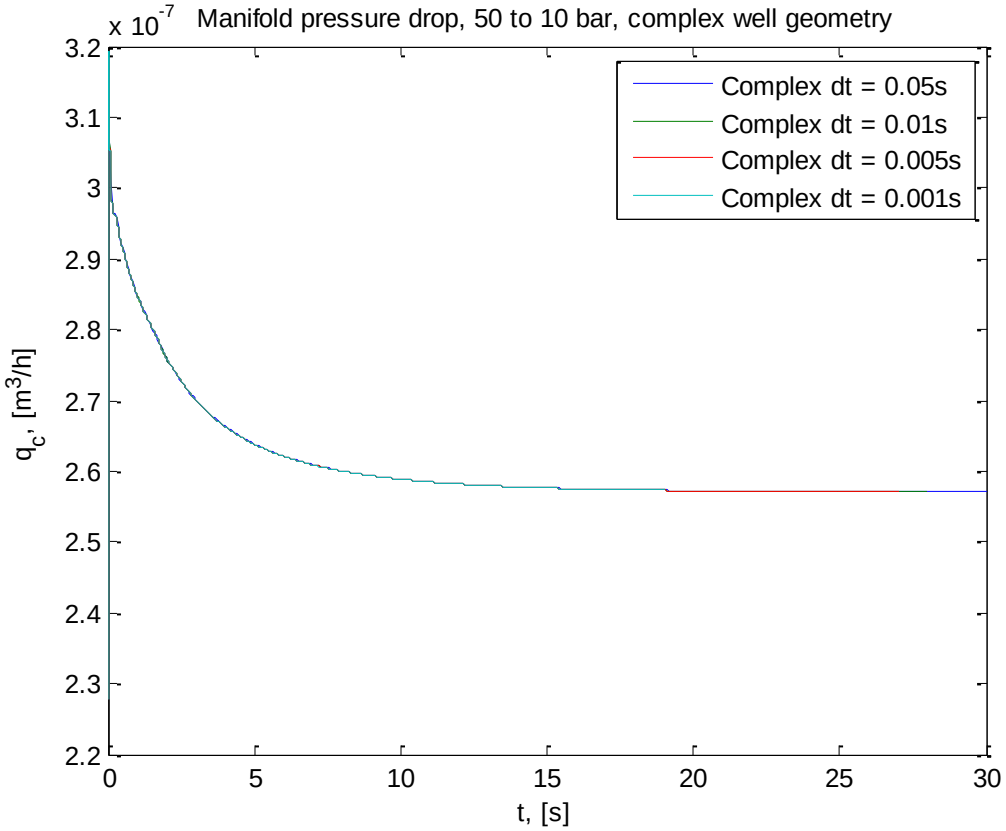

Figure 12: This figure shows the time development of the choke flow after a sudden decrease in the manifold pressure for different time steps.

6.3.4 *Mapping of pressures and flows*

The function containing the differential equations needs all input and output variables as one vector. This means that both flows and pressures in the control volumes must be stored in the same vector, and the same is valid for their derivatives.

In the simple single well model, the two pressures are contained in the two first elements, while the single flow is stored in the third element.

In the complex single well model, the pressures and flows are organized in a large vector in the following way:

$$[\ d\bar{p}_1/dt, , , , d\bar{p}_{m+n}/dt, d\bar{q}_{m+n+1}dt, , , , d\overline{q_{2m+2n-2}}/dt\ ]$$

m+n elements, m+n-2 elements

All the pressures are stored in the first $m+n$ elements, and all the flows in the next $m+n-2$ elements.

For the multiple well model, the manifold pressure is stored in the first element of the large vector. The well variables are then stored in blocks of three, where the first two are pressures and the last one is flow.

6.3.5 *Other comments on the implementation*

Here, we will just make some comments on the implementation that may be useful for the user to know.

The basic integration time step is given by the variable `dt` in the programs. *All* other time quantities, such as the time scale in plots and control time intervals for the ESP and the choke, should be an integer number of this time step. If this is not the case, errors may occur.

The plotting interval, meaning how often to update the figures, must be chosen less than or equal to the smallest control time interval. For example, if the ESP is controlled every second, the plots have to be updated every second or more often. Alternatively, deactivate all plotting in order to speed up the calculation.

The amount of data produced by the calculation will get huge if the program runs for a long time. To avoid heavy memory consumption, old data will be deleted by the program. There are three variables describing this:

- Data history (dense): For how many seconds after the current time all data should be stored. For example, if this is set to six seconds, then all data will be kept for the last six seconds of the simulation.
- Data history (sparse): For how many seconds after the current time some data should be stored. For example, if this is set to 120 seconds, some data is stored in the previous 120 seconds, but all data older than 120 seconds is deleted.
- Time step, sparse data: This is the desired time step in the sparse data. For example if this is set to 1 second, only data from every second will be stored in the sparse data time interval.

User provided inputs in the GUIs are updated every time the plots are updated. Changes in the PI index, reservoir pressure and downstream choke pressure in the one well GUI will be discrete, but changes in the frequency and choke opening are made smooth by the program. See the section on ESP and choke transitions under control.

If the user presses the “Stop simulation” button, *all* variables involved in the calculation that are not deleted will be stored in the GUI folder by the name `data.mat`. The user can press the disk button in the top left corner of the GUI in order to choose where to store

the data. However, then only the calculated pressures and flows in addition to the environmental variables and user input are stored.

Both the single well simulation program and the N wells simulation program are modularized in such a way that components can be easily switched out by others. For example, the calculation of friction is done in a separate function that can easily be replaced by a different one. Changing the ESP and choke characteristics is also easy, and the method for doing so is described below.

How to change parameters, well geometry, ESP characteristics and choke characteristics is described in the appendix. A general description of the purpose of the functions in the different folders is also given there.

7 Simulation results

7.1 Transition analysis

It is important to analyse the transition behaviour of the different models in order to understand the occurring phenomena and to find a compromise between accuracy and simplicity especially with regard to the purpose of controller design. The possible transitions can be triggered changes of the environmental boundary conditions, e.g. the choke output pressure or the reservoir pressure. Arbitrarily the latter was chosen and a

sudden transition from 100 bar to 150 bar simulated. An almost instantaneous transition of that magnitude is highly unlikely but should be suitable to show the possibilities and limitations of the different models. The program that produced the plots in this section is located in the folder “Transition analysis”.

7.1.1 Sudden change of the reservoir pressure

The simulation was run for different system setups, i.e. number of states in the complex model.

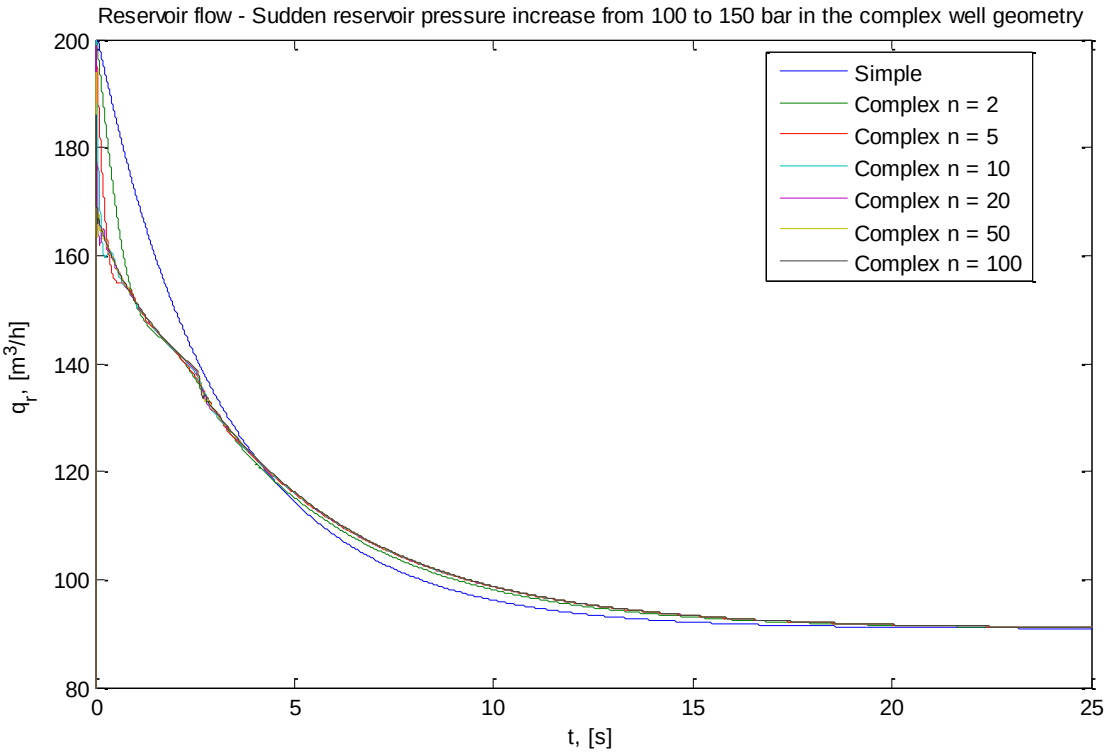

After a strong instantaneous increase the reservoir flow decreases towards a new steady state in a period of about 20 seconds after the disturbance. While the simple model shows a smooth decay, the complex model shows a stronger decrease in the beginning and a slightly longer relaxation time. Additionally this general behaviour is overlaid by oscillations which will have to be discussed in more detail. Comparing the flows for different system dimensions it can be stated that with increasing number of states the solutions of the complex model converge.

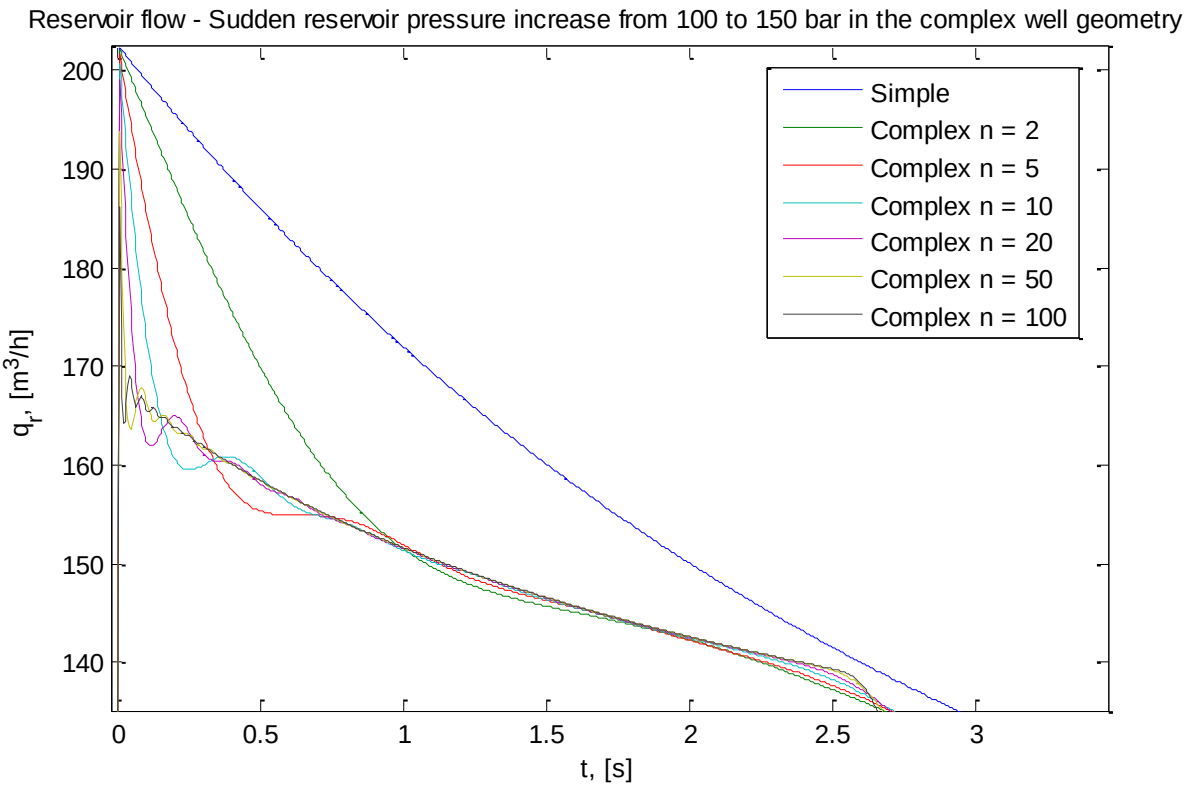

This zoomed cut-out of the original plot gives a better insight into the differences between the models and the converging behaviour. The higher the number of control volumes in the complex model is, the sharper is the decrease after the disturbance. The sharp transitions excite small oscillations whose frequencies also depend on the length of the chosen discretization. These oscillations result from instantaneous changes and do not occur in continuous transitions as shown in the analysis of a continuous transition below. As they are dependent on the spatial discretisation their origin is numerical and not physical. Though their magnitude is negligible and therefore a further analysis is not needed.

Around 2.5 seconds after the disturbance the complex model shows another oscillation which results from the reflection of the pressure wave at the ESP. The pressure wave travels with the speed of sound, i.e. 1274 m/s for the chosen constants which is the expected behaviour. Physically, this suggests that the effect of the disturbance should reach the pump and the choke with a delay.

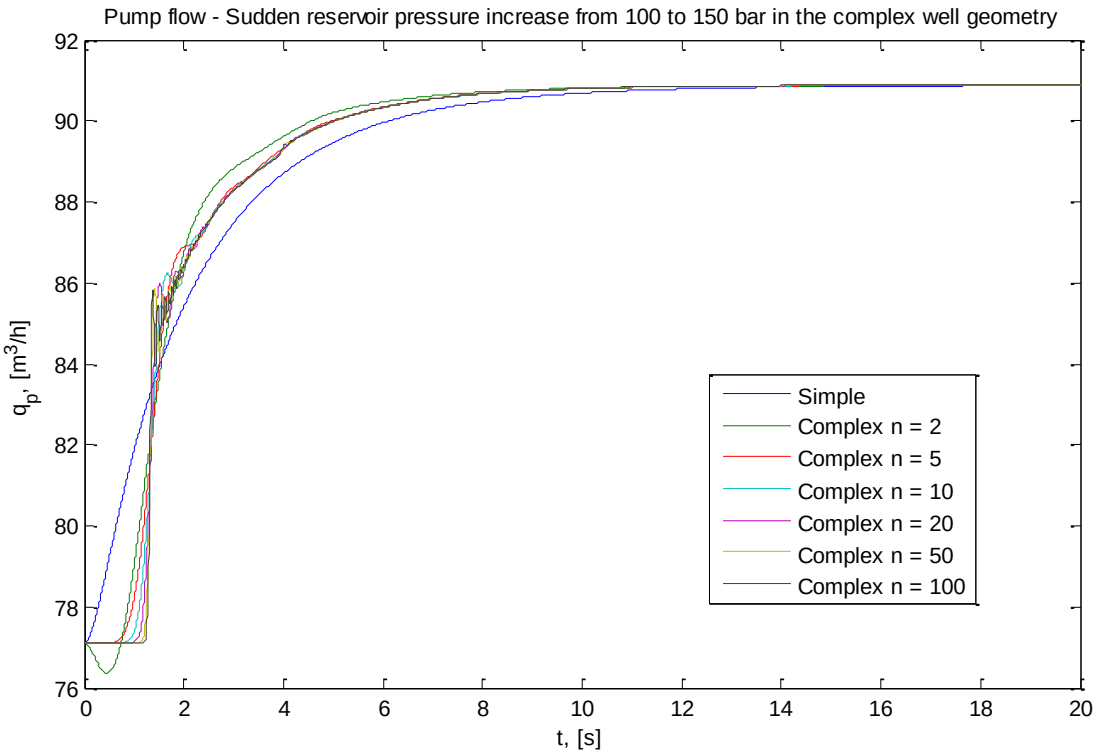

As one can see from this plot the pump flow increases within the same period to the new steady state. Again the simple model shows a smooth transition. This transition starts immediately and does not show any delay. Since the propagation speed of the disturbance is finite this behaviour is not physical.

The complex model takes this delay into account. Again the general behaviour is overlaid by oscillations which arise from the discontinuous transition and again the complex solution converges with increasing number of states.

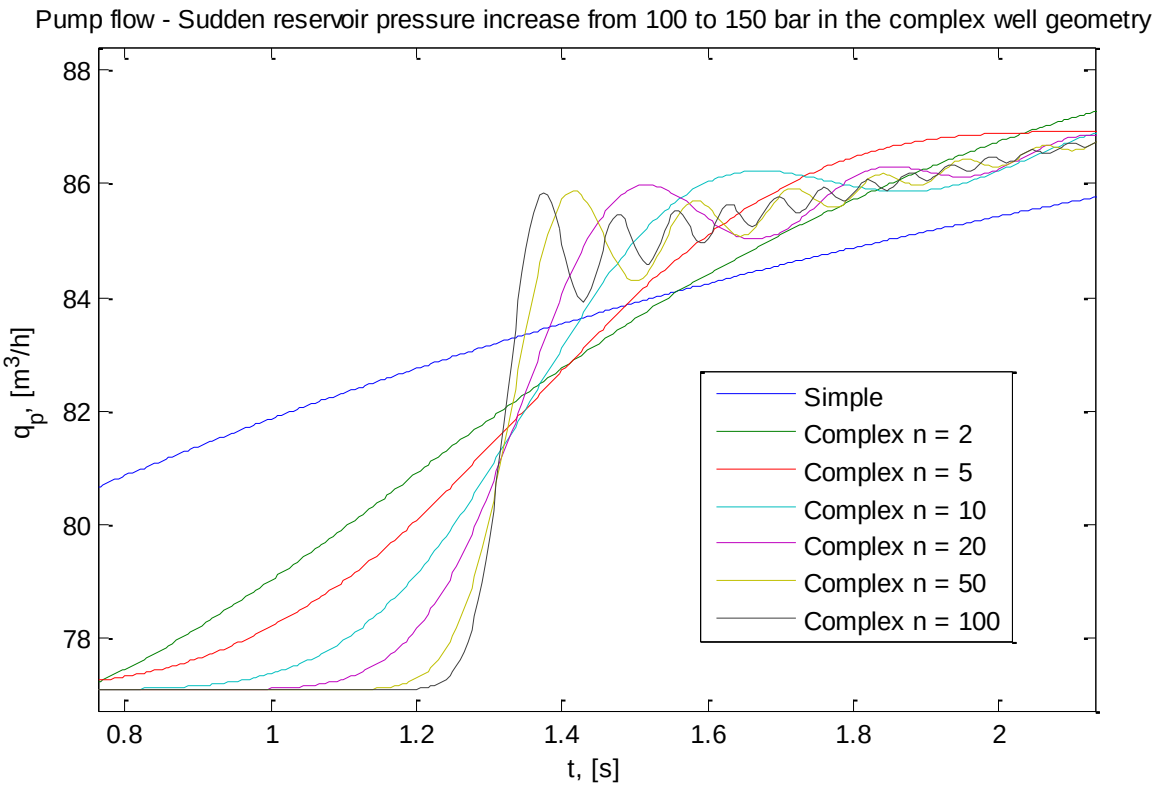

As shown in the figure above the length of the delay depends on the number of control volumes but also this value converges with increasing number of states.

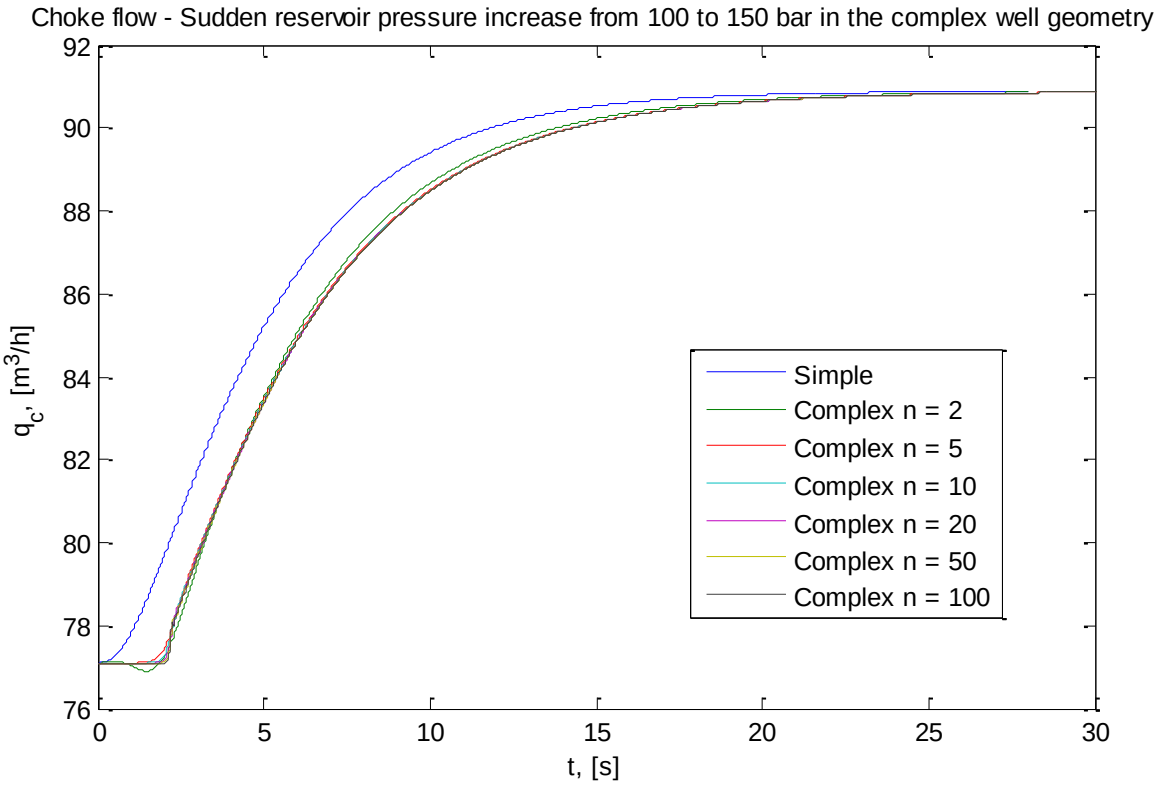

In the simple model also the choke flow reacts without any delay. As already discussed this behaviour is not physical. The complex model converges and behaves as in the examples above and takes this delay into account.

The new steady state reached is the same one found by initialising the system with the new boundary conditions.

7.1.2 Manual ESP transition

A different transition behaviour occurs if the system is not disturbed by instantaneous changes but by continuous transitions. If the ESP-frequency is changed it takes some time for the hardware to react which is taken into account by continuous transitions in a finite time.

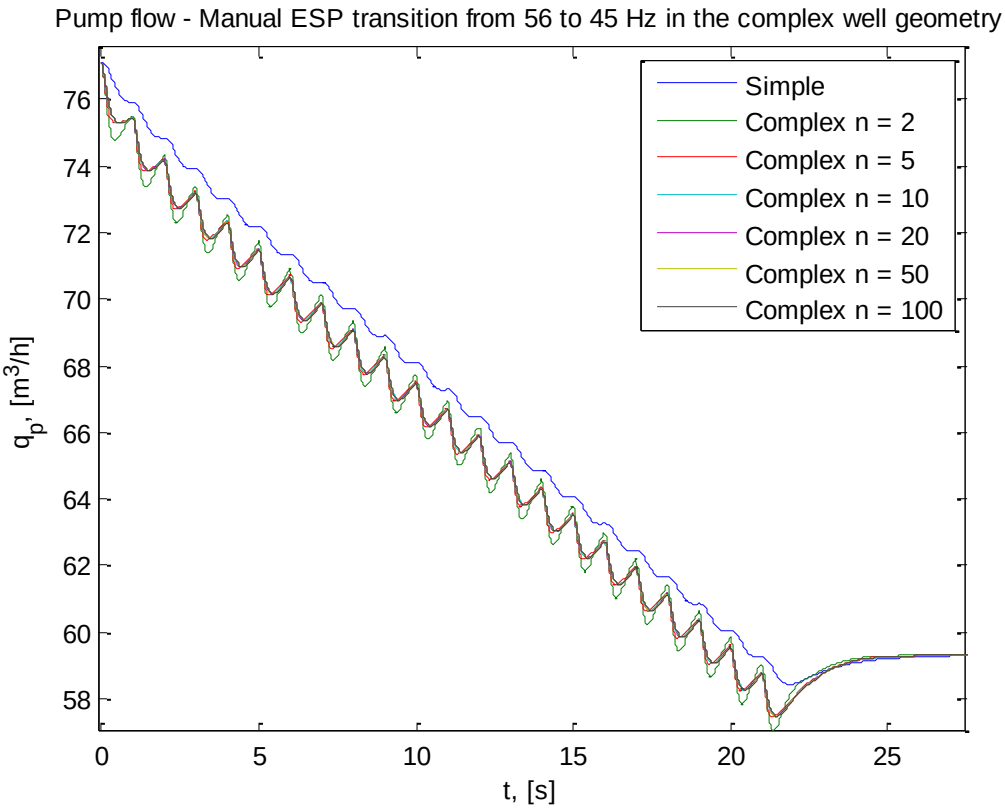

In the plot above the pump flow for a manual frequency change from 56 Hz to 45 Hz is shown. As already discussed the continuous changes do not trigger an oscillating overlay in the complex model such that both models evolve smoothly, though the simple and the complex model differ. In the simple model the effect of the frequency change on the actual local pump flow is reduced since the overall system friction is smoothening everything. In the complex model the actual local behaviour at the ESP is described properly. Due to the different rates of frequency transition the flow is first decreasing and then increasing again. This effect arises from two opposing effects whose strength changes dependent on the rate of change of frequency. The first effect decreases the flow: Due to the change in frequency, the characteristics are changed. On the characteristics for the (new) lower frequency the current pressure difference results in a reduced flow. This can be visualized by a movement to in the characteristics-diagram in parallel to the flow axes in decreasing direction. The second effect increases the flow: Due to dynamics, the decreased flow from the first effect results in a decreased pressure difference. A decrease of the pressure difference on a constant characteristics leads to an increase of the flow. This effect can be visualized by a movement on a constant characteristics towards a higher flow.

At the beginning of a frequency transition step, the rate of change in frequency is quite high. Therefore the characteristics used in the calculations change rapidly and the first

effect is dominating. At the end of the transition step, the frequency is almost constant. Therefore, the second effect will start to dominate. As discussed in the section about the ESP-implementation, this behaviour depends on the shape of frequency transition. Anyway, the complex model captures the actual local behaviour, which is not possible in the simple model.

7.2 Accuracy conclusion

The simple dynamic model is accurate enough to show much of the general system behaviour. However, local behaviour and propagation speed may be important, for example at the ESP, and then the complex model is needed.

For the complex model, the converging behaviour does not give rise to a clear result. For example, to capture the delays completely, at least 50 control volumes in each tube should be chosen. Except for this, all the effects in the complex model are already captured by e.g. 10 control volumes in each tube. This accuracy should be enough for most purposes.

7.3 Simulation of the start up of an ESP in a *N* wells system

Assume that N wells are connected to a manifold, and $N-1$ of them are operating in a steady state while the choke for the last well is closed and the ESP shut down. A possible scenario one wishes to simulate is to then start the last ESP and see how this affects the other ESPs. This is not possible to simulate in our model.

When an ESP is shut down, the well will contain water, oil and gas, and because of differences in density, these phases will not be mixed, but separated in the steady state with the water at the bottom, the gas at the top and the oil in the middle. However, throughout the model presented here, a pseudo single phase liquid in the well is assumed. This means that in order to do the full simulation further extensions of the models presented here are needed, i.e. a gas phase or an annulus has to be added.

However, a similar but less complicated scenario can be simulated with this model. If all the ESPs are working, but one is working on the lower frequency limit, which is 35 Hz, the frequency of this ESP can be increased to a higher one. The effects of this change in the other wells can then be investigated.

An example of such a simulation is given here for a system consisting of two wells. The ESP characteristics are shown in *Figure 13* to Figure 15. Here the ESP in well 1 is held at a constant frequency of 56 Hz while the frequency of the ESP in well 2 increases from 35 Hz to 56 Hz in 14 seconds.

From the figures, one sees that the all the flows in the second well increases. At the same time, the pressures above the ESP increases, and the pressures below the ESP decreases.

This happens because the increased frequency of the ESP in this well produces a larger head, and thereby a larger flow.

The second well is severely affected by the changes in well 2. The simulation was carried out with a constant booster pump flow, so that an increased flow into the manifold from well 2 will necessarily cause a decreased flow in well 1. At the same time the ESP in well 1 is held at a constant frequency, and this causes the head provided by the ESP to increase. The decreased flow causes an increase in the flow bottom hole pressure (from the PI equation), that in turn causes increased pressures below the ESP. This, combined with the increased head provided by the ESP results in the increased pressures above the ESP.

From *Figure 13* one can see that the ESP does not move outside the operation envelope, but this could easily happen in a different scenario. Therefore, control is needed to keep the ESPs inside the operational envelope.

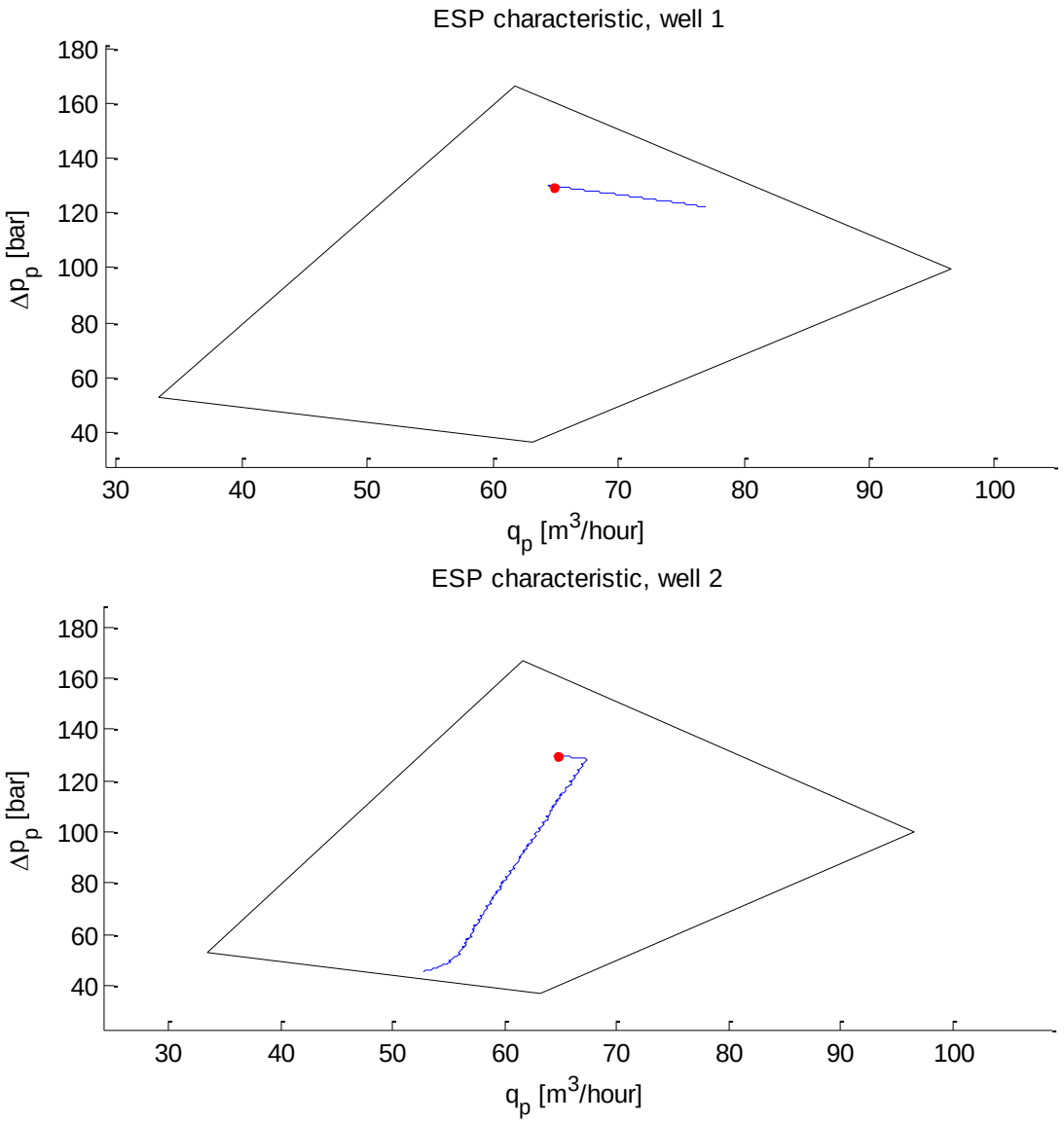

Figure 13: This figure shows the ESP characteristics for the two wells during the transition.

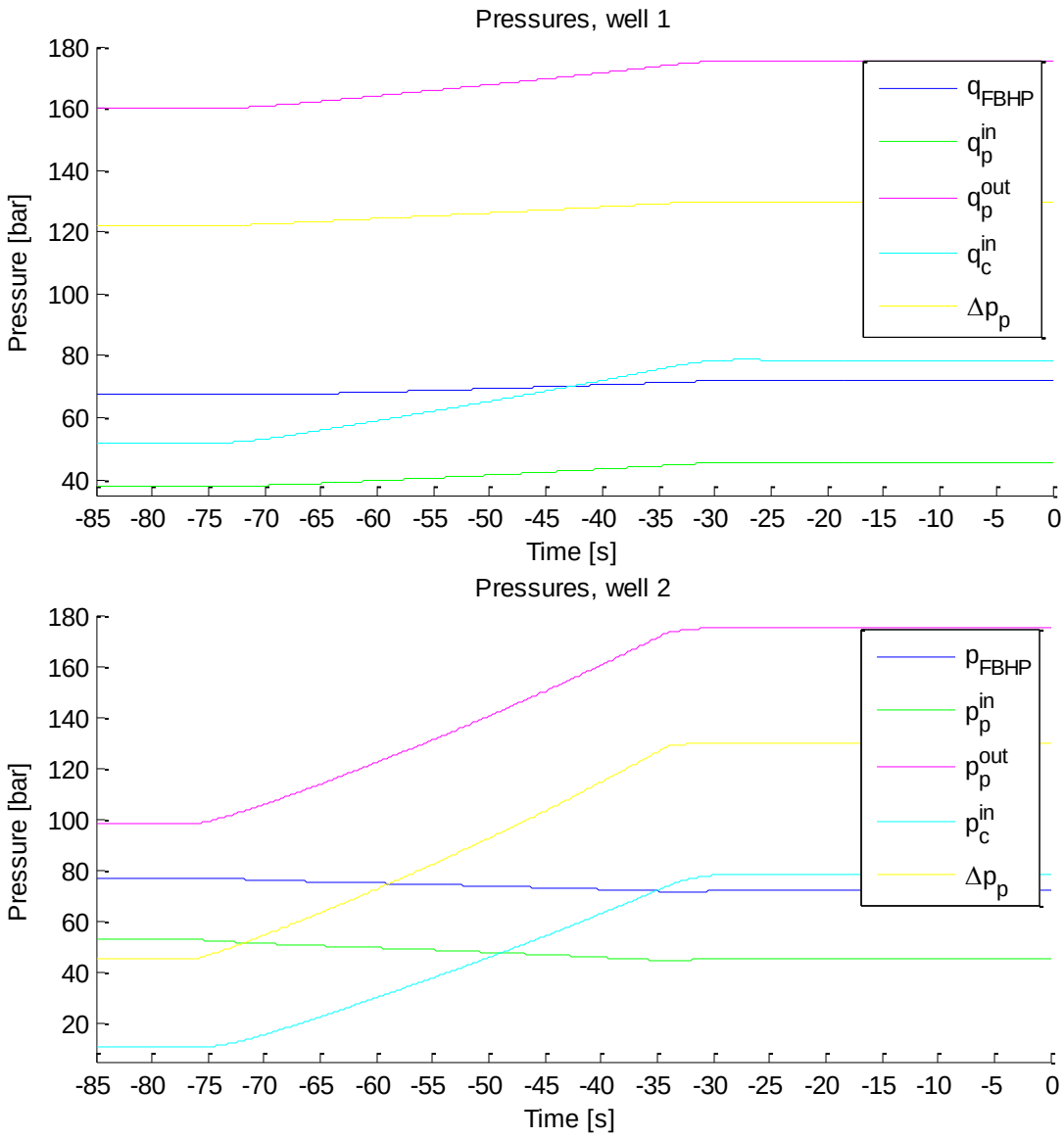

Figure 14: These figures shows the pressures in the two wells during the transition.

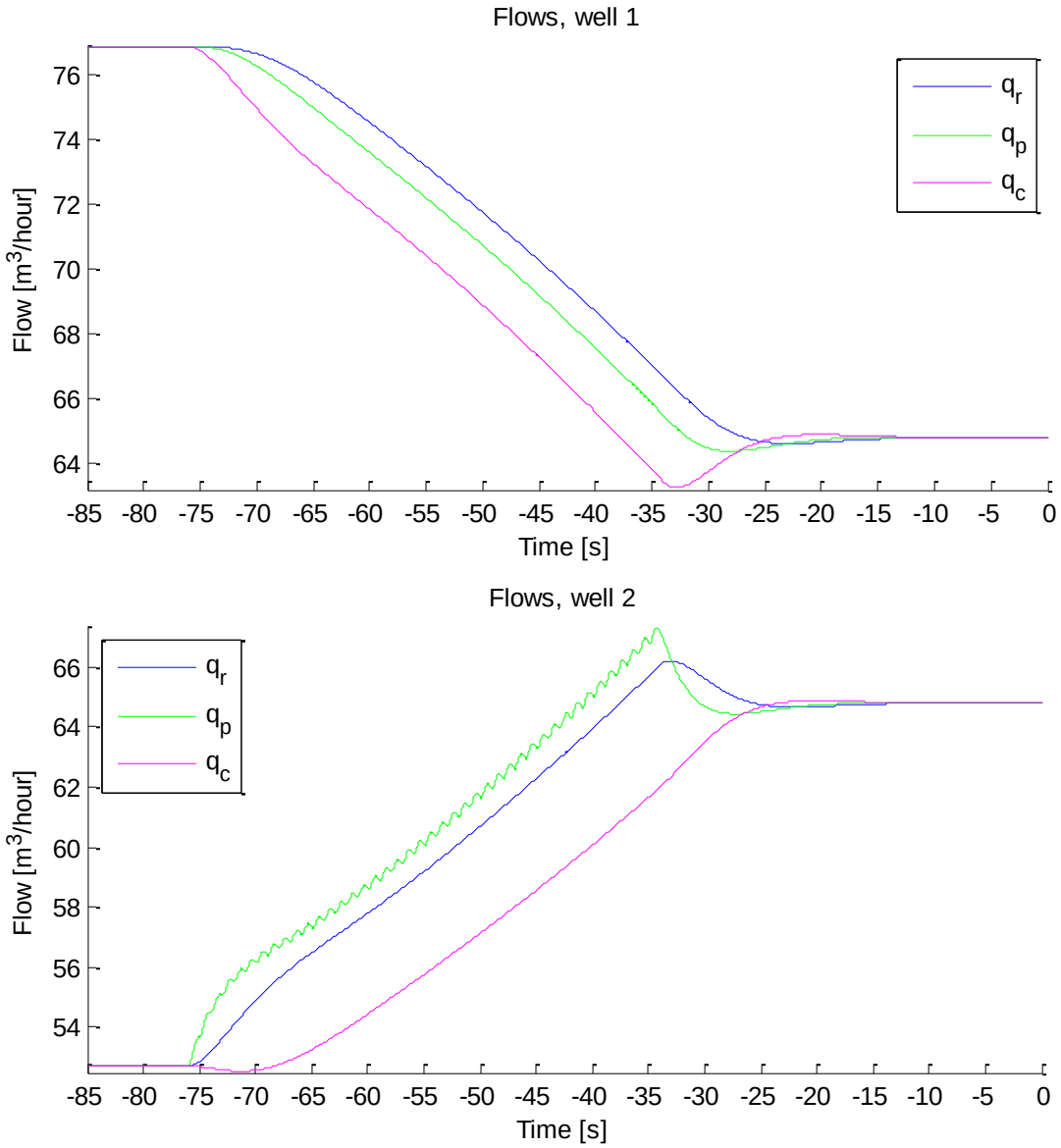

Figure 15: This figure shows the flows in the wells during the transition.

8 Control for single well dynamic model

8.1 System overview

The whole system includes three main parts: GUI (user interface), Mathmatic Model and Control loop. How the control loop is working explained in this chapter.

8.1.1 The control objects

In this project, since we are curious about the pressure drop that ESP pump produces, which is also the main element influences the productivity, and we also care about the flowrate which is mostly related to the safety and efficiency of ESP pump, excepts the pressures, the main control objects are decided as the dp (pressure drop) and q_c (choke flow, which is similar with flow through ESP, q_p).

8.1.2 The control variables

For the ESP pump, the control variable is frequency, because the power of ESP is related with frequency.

For the Choke, the control variable is Choke opening (the position how much the choke opened), because the choke is similar with a valve.

8.1.3 Control flow chart

The Figure 1shows the work flow of the control system. In this project, the control loop is a simply feedback loop. Firstly, the operators can define the properties and initial conditions of the whole system, such as the speed of the progress, initial ESP working frequency and so on. With these conditions, the mathematic model simulates the dynamic status which also produces the process values to controller.

Then, the operators give desired setpoint of pressure drop throughout the ESP and the setpoint of flow that can be controlled by choke opening to the Controllers in GUI.

Finally, the controller calculates and gives out control signal of frequency and choke opening to dynamic model to change the status of process. This how the feedback control loop is formed. The main controller of this system is called *combined control*, and it includes two parts. One controller for ESP and another controller for choke. Each controller consists of a region controller (PI controller), a quantizer and a transition. Operators can choose to use manual control (give control signal directly) or to use automatic control (PI controller)

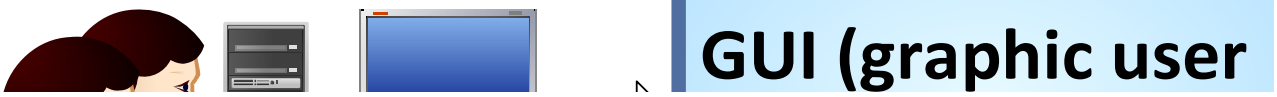

Figure 1 Flow chart of control system

8.2 Region Control

There are some safety and working efficiency problems of ESP which should be considered, for example if the pressure drop is too small and the flow is too big, the ESP might be damaged, another example is if the ESP keeps working with high frequency, the temperature over the pump might be too high for the oil, and correspondingly causes a fire hazard. This kind of damage and fire disaster absolutely should be avoided. To make ESP working life longer, it is required to main it working under a safe and ideal condition that correspond to the flow trough ESP and the pressure drop through the ESP.

In this project, we just considered the ESP working constrains for flow rate and the pressure drop. The temperature control is not included.

8.2.1 ESP Working constrains

A typical working constrain depends on three different water cuts can be seen Figure 2. These constrains are gained from data sheet of HC2000 64 stages ESP pump. With these data, other constrains depends on a different water cuts are developed.

Maximum working rate of ESP is 1000KVA or 65Hz in this project. Minimum working rate is 35Hz. These two characteristic curves depend on the properties of ESP. The downthrust and upthrust curve are the maximum and minimum ratio of Head and Flow that make the ESP working at a good condition.

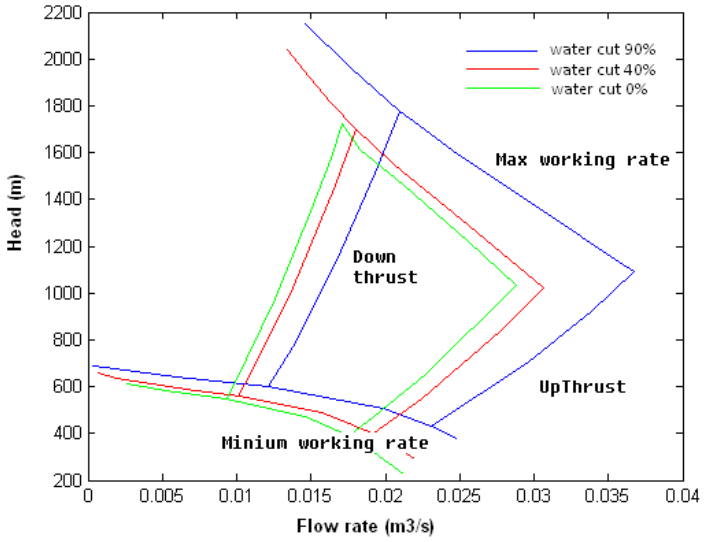

Figure 2 Safe working region depends on water cut

In the Figure 3, it shows how the constrains depend on different water cuts achieved. First, we connected the four main points of every two different water cut constrain curves with linear lines, as shown as the black lines in figure 6.3. Then divided these lines equally into 50 elements (or whatever you want). When input the water cut to the subfunction *constrains*, it will evaluate this water cut is at which element. Then connect the same elements at the four black lines to get the constrain area as a quadrilateral, as shown as brown lines in Figure 3. For example, if the water cut is 65% and the black lines are divided to 50 elements, then 65% is at the 25th point. Connect the four 25th points, and we got the constrain area for water cut 65%. This is just a simple treatment for the working limitation of ESP in different water cut liquid, since there is no existed reliable mathematical model for this ESP constrain. And this work is done in the subfunction called *constrains*.

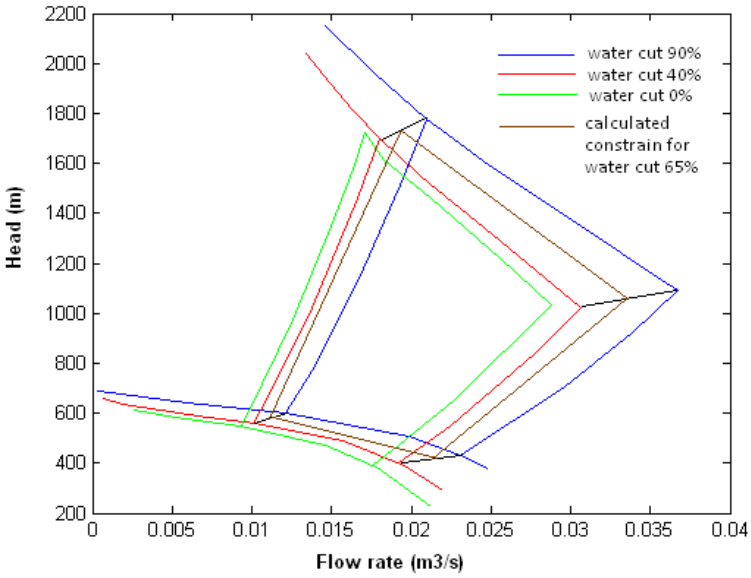

Figure 3 Result of calculating working region for 65% water cut

8.2.2 PI controller

PI controller equation

ESP:
$$f = K_{P\_ESP} \cdot e_{dp} + K_{I\_ESP} \cdot \int e_{dp} \cdot dt$$
$$e_{dp} = SP_{dp} - PV_{dp}$$

Choke:
$$z\_c = K_{P\_choke} \cdot e_{q\_c} + K_{I\_choke} \cdot \int e_{q\_c} \cdot dt$$
$$e_{q\_c} = SP_{q\_c} - PV_{q\_c}$$

Where SP is setpoint, PV is process value, Kp and Ki are PI controller parameter, f is frequency, z_c is choke opening.

The PI controller is embedded in subfunction *regioncontrol*. The work flow for the region control is shown in

Figure *4*. In the region controller, the setpoint is given by operators. The process values are given by mathematical model simulations, which contains flow rate, pressure, choke opening, ESP frequency. The working constrains are given by subfunction *constrains.*

When the process values are in the ESP safe working region, the PI controller will be activated. And PI controller will produce the control signal as frequency and choke opening automatically. When the process values are out of the safe working region, the region control function will firstly send a warning to the operators and guide them what to do. At the same time, it will maintain the frequency or choke opening as what they

were at last time step. For safety consideration, it is better for the operators follow the guidance as soon as possible.

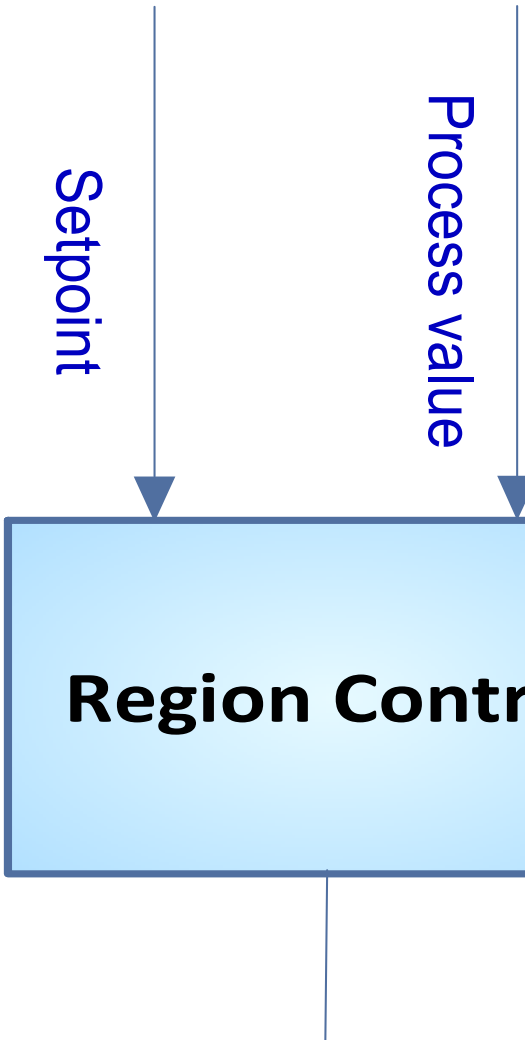

Figure 4 Region control flow chart

Tuning PI controller

This project used the Ziegler-Nichols method to tune the PI parameters.

Tuning process:

1. Tune the controller to Kp-only model, turn off the Integral modes off

2. Tune the controller gain Kp up slowly and observe the output response. When a value of Kp results in a sustained periodic oscillation in the output (or close to it), mark this value as Ku. And the period of oscillation as Tu (time out).
3. Using the Ku and Tout to calculate Kp and Ki with the table below.

PI control	$K_p = K_u/2.2$	$K_i = T_u/1.2$

Because there are two PI controllers in this project, we firstly tune one, then turn it off and tune the other one. The final values of these parameters are different with those gained by Z-N method since the interaction of these two PI controllers. There are also some adjustments did to make the model stable. Finally, these parameters are

$$K_{P\_ESP} = 3 \times 10^{-7}, K_{I\_ESP} = 1.2 \times 10^{-7}$$

$$K_{P\_choke} = 340, K_{I\_choke} = 1200$$

8.3 Quantizer and Transition

The quantizer and transition are made to simulate the real control signals. The control signal output from the controllers is a step change. But it is not real in the industry. The choke can move three seconds for 1% position change and then stop 3 seconds before next move. The movement of choke opening and time is a linear relation. An actuator can send a control signal of 0.5 Hz every second to ESP. This signal and time are nonlinear relationship. We used a second order filter to simulate the frequency signal

Choke: the quantizer subfunction makes the maximum change of choke opening as 1% at every step. The transition subfunction makes the opening change as a linear line and stop

moving every 3 seconds. The result of changing choke opening from 100% to 96% can be seen in Figure 5

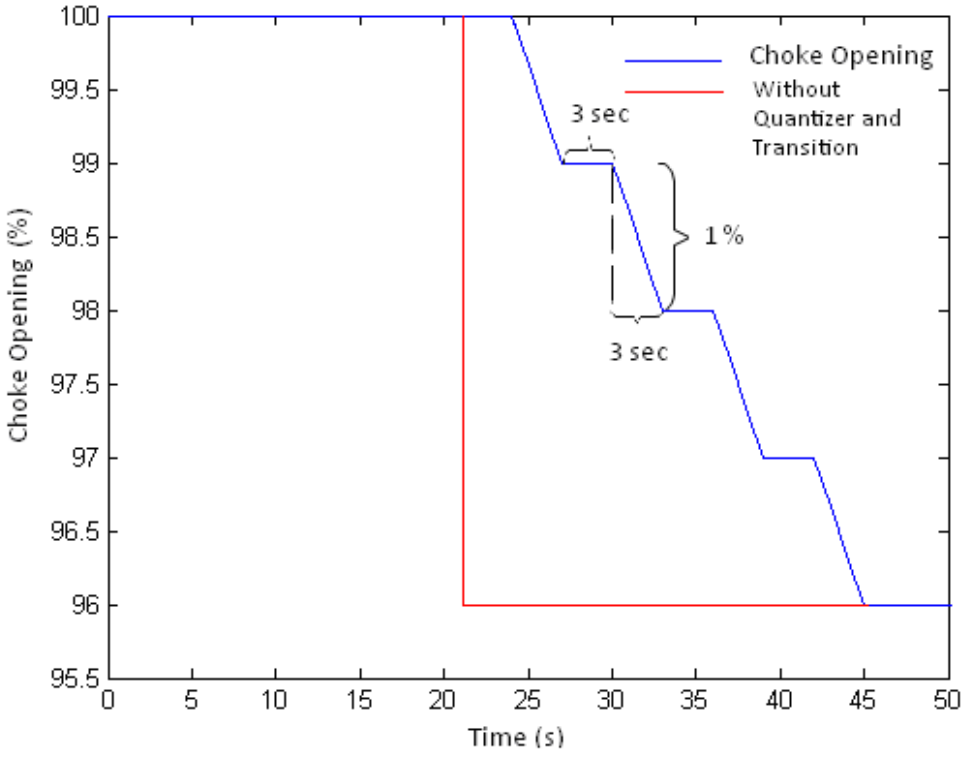

Figure 5 Simulated choke opening

ESP: the quantizer subfunction makes the maximum change of frequency as 0.5 Hz at every step. The transition subfunction makes the frequency change as a second order filter. The equation is

$$f = (\frac{1}{\tau}) \cdot (e^{-t/\tau} \cdot (\tau \cdot (f_{new} \cdot (e^{t/\tau} - 1) + f_{old}) + t \cdot (f_{old} - f_{new}))$$

Where τ is filter constant, f_{new} is the output of quantizer, f_{old} is the frequency of last time step.

The result of changing choke opening from 56 to 52.5 can be seen in *Figure 6*. The result of one step change can be seen in Figure 7.

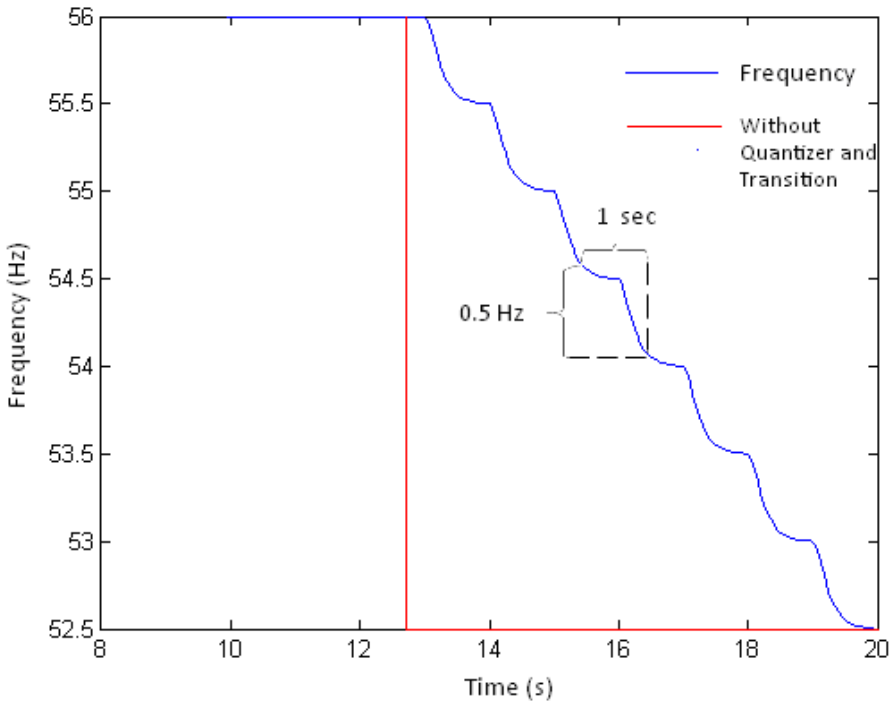

Figure 6 Simulated frequency change of ESP

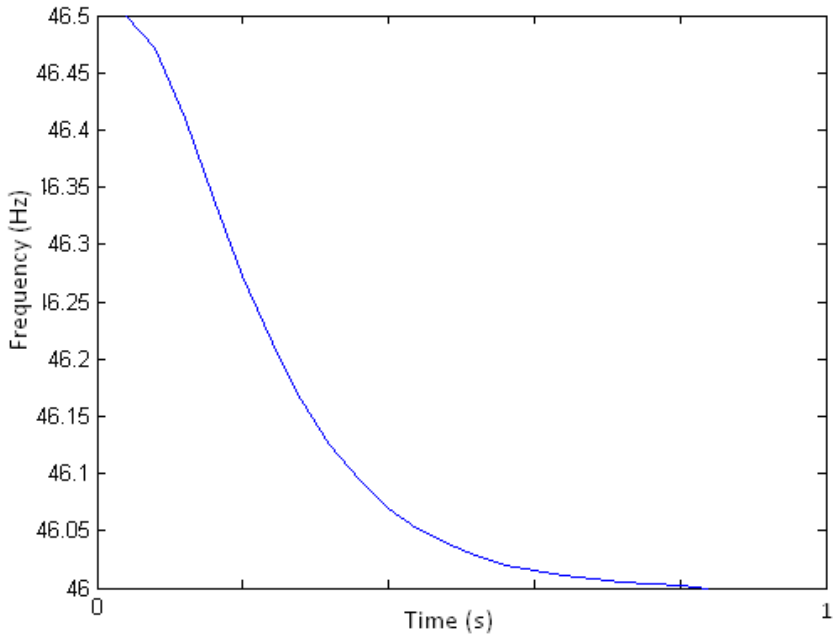

Figure 7 Simulated one step change of frequency of ESP

8.4 Control simulation results

The performance of the control systems should be tested for these purposes:

1. How it reacts with environmental disturbances, such as step changes of choke pressure. This is mostly related with the performance of PI controllers.
2. How it reacts with undesired operations, such as give a setpoint out of safe region, or unsafe manual control. And how it reacts with big disturbances. This is testing the function of region control.

8.4.1 Testing PI controllers with different setpoints

1. Activate automatic control for both ESP and Choke

2. Change the setpoint of for dp = 80 bar, q_c = 60 m3/hour to dp = 100 bar, q_c = 80 m3/hour, and then to see the performance of PI controllers.

Result:

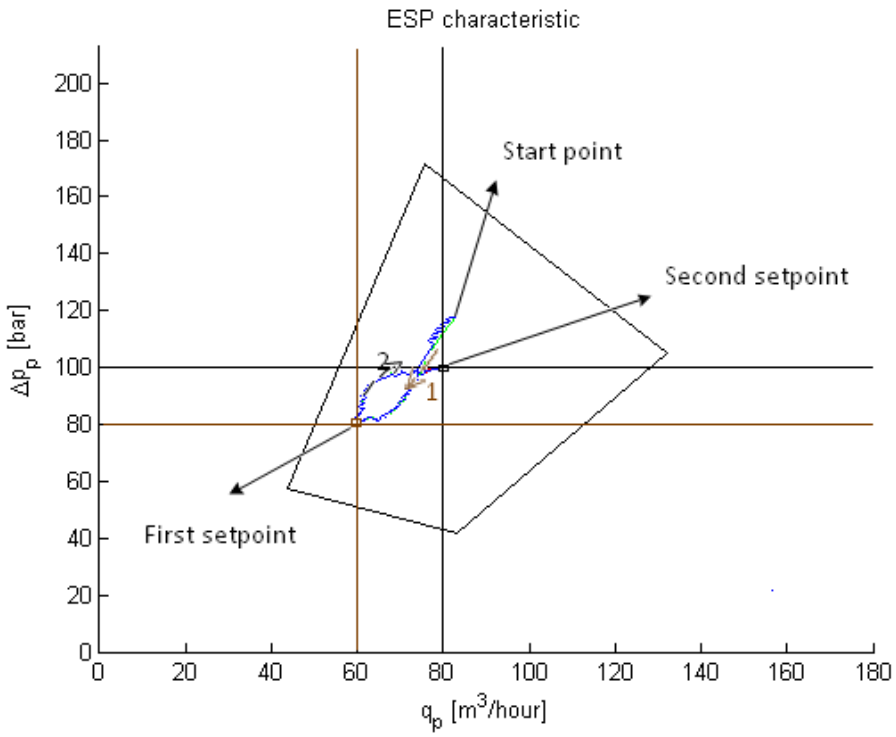

Figure 8 Testing result of changing setpoint

Comments: we can see the process was tracking the setpoint very well. The PI controllers works.

8.4.2 Testing PI controllers with disturbances

1. The main disturbance for one single well mostly from choke downstream pressure. Change the choke downstream pressure from 20 bar to 40 bar. Setpoint for dp is 80 bar, setpoint for q_c is 60 m3/hour.

   Result:

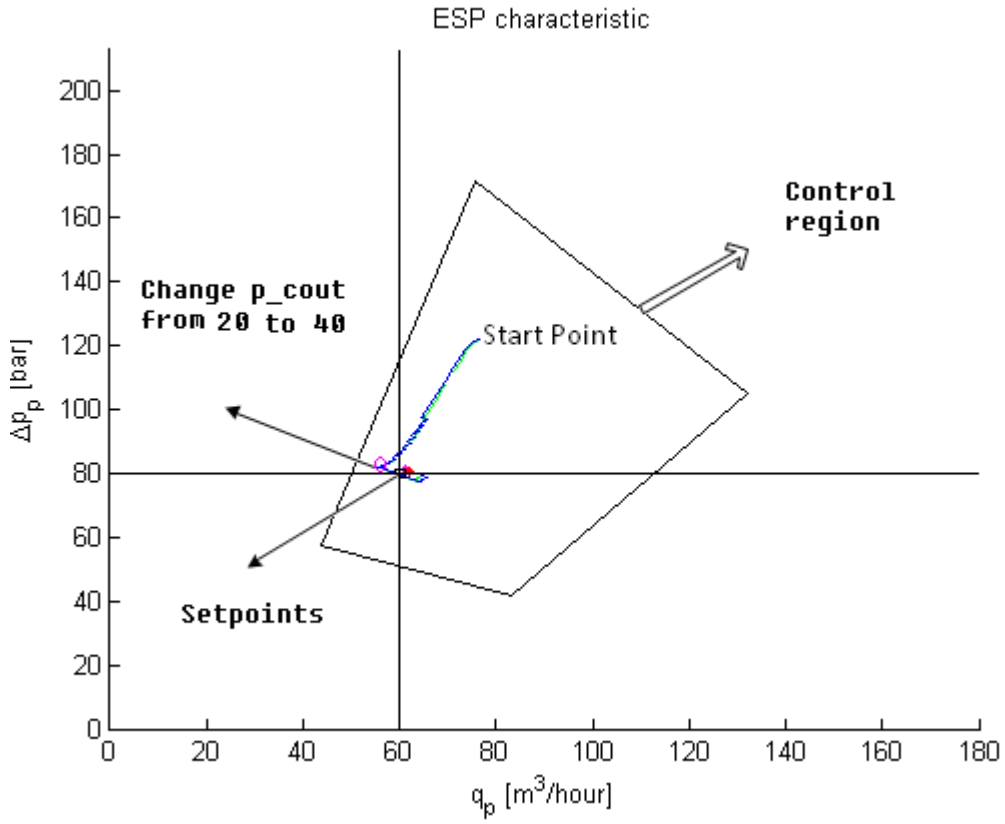

Figure 9 Testing result of adding disturbance

Comments: After gave a disturbance of 20 bars, the process still can track the setpoint, and there is no big unstable response, it proved the ability of affording disturbance of PI controller OK.

8.4.3 Testing region control

At an arbitrary point, we gave a big disturbance as 40 bar change of the choke downstream pressure to force the process point go out the safe region.

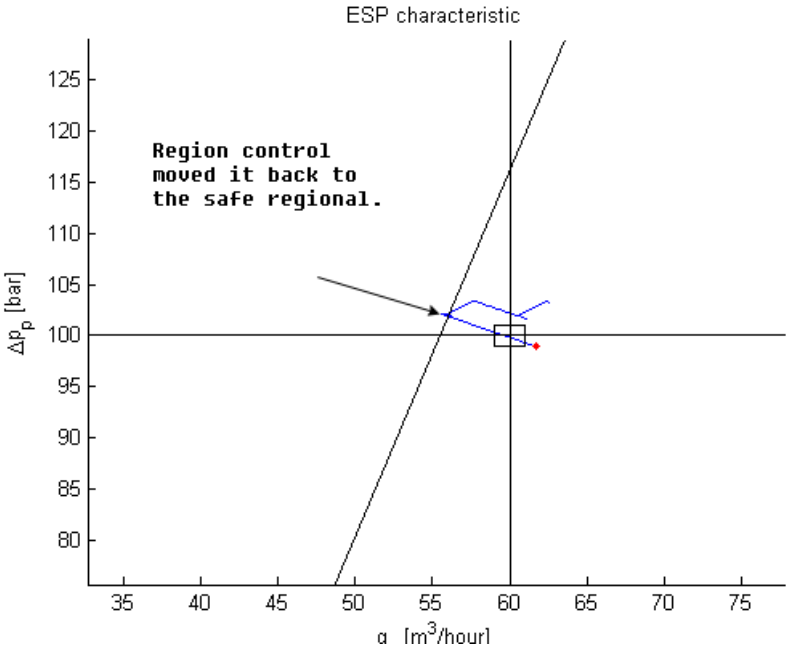

Figure 10 Testing result of region control

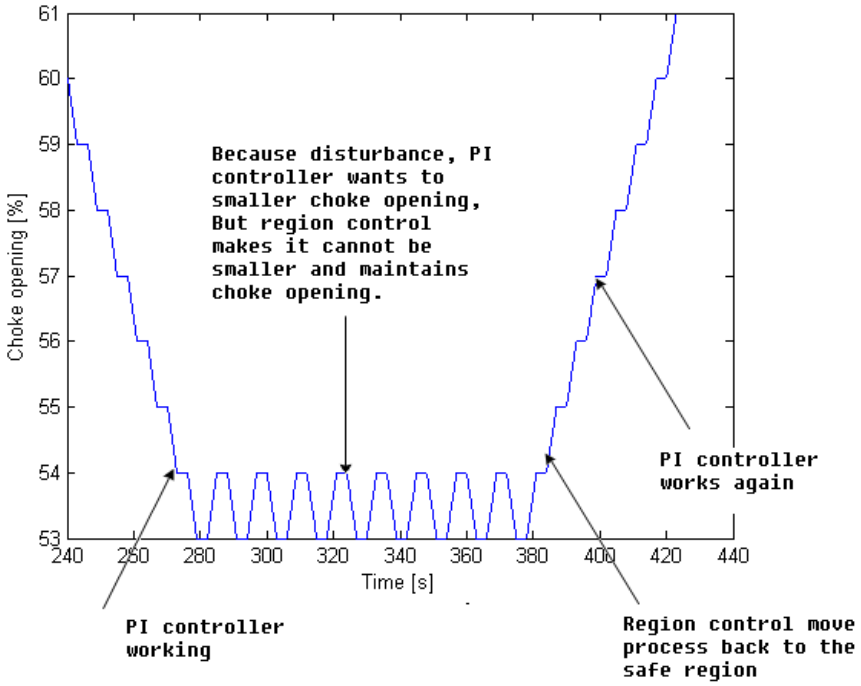

Figure 11 Testing result of control signal of region control

The results of how the control signal behavioured and the ESP characteristics plot shows the region control can move process back to the safe region.

8.5 N-wells control system

In this project, the N-wells system includes a production manifold and two wells. There is a boost and a water inlet valve need to be controlled in the manifold. Here is an overview of the N-wells system. The flow and pressure of the wells effect the situation in the manifold and the same in the reverse way. At present, we just added region control functions to the well1 and well2, the boost pump and the water inlet valve are manually controlled.

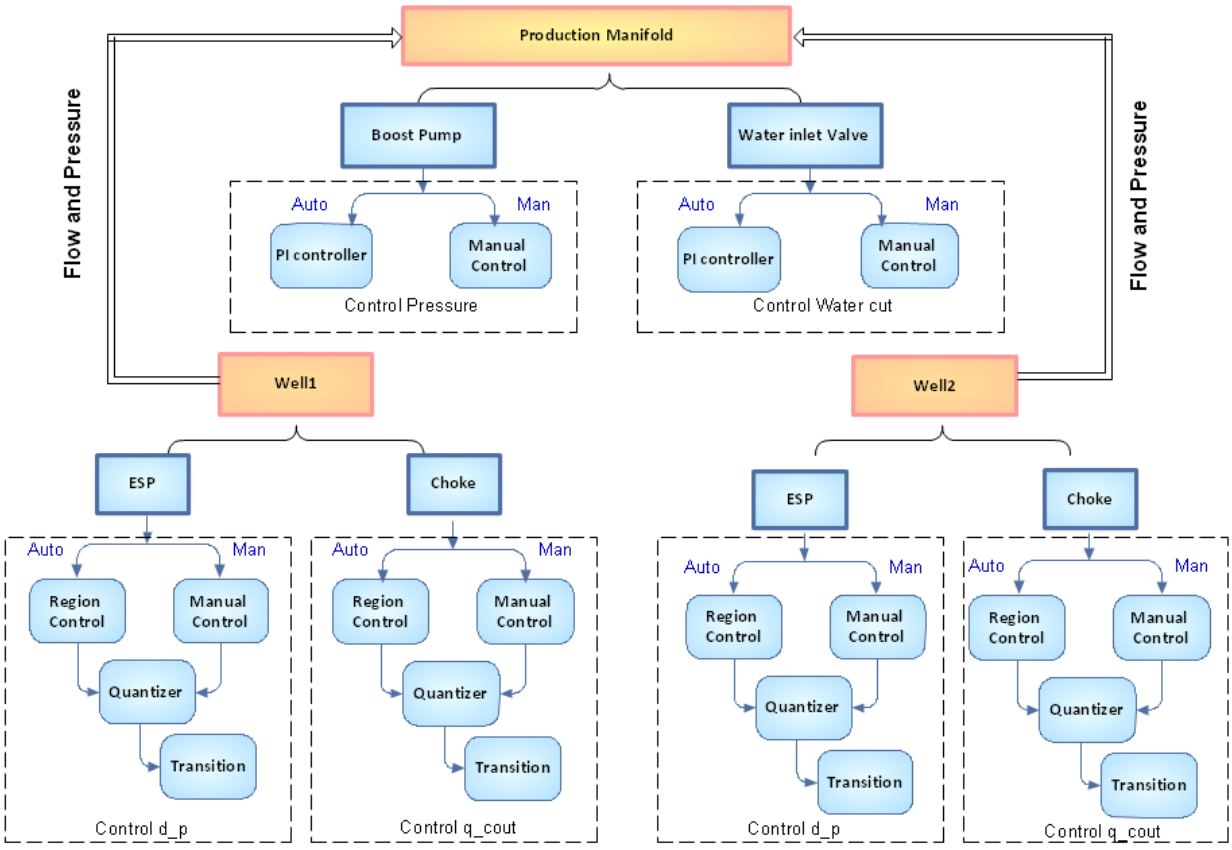

Figure 12 Flow chart of N-wells control

8.5.1 Simulation results of N-wells system

Form Figure 13, we can see with the PI controllers, the two wells process can track the setpoint. But the flows of the wells affected each other. When the flow in well1was increasing, the flow in well2 l decreased. This is reasonable, because of the flow out of the boost pump of day, which equals to total of two wells flow and water inlet flows, is a constant at this time.

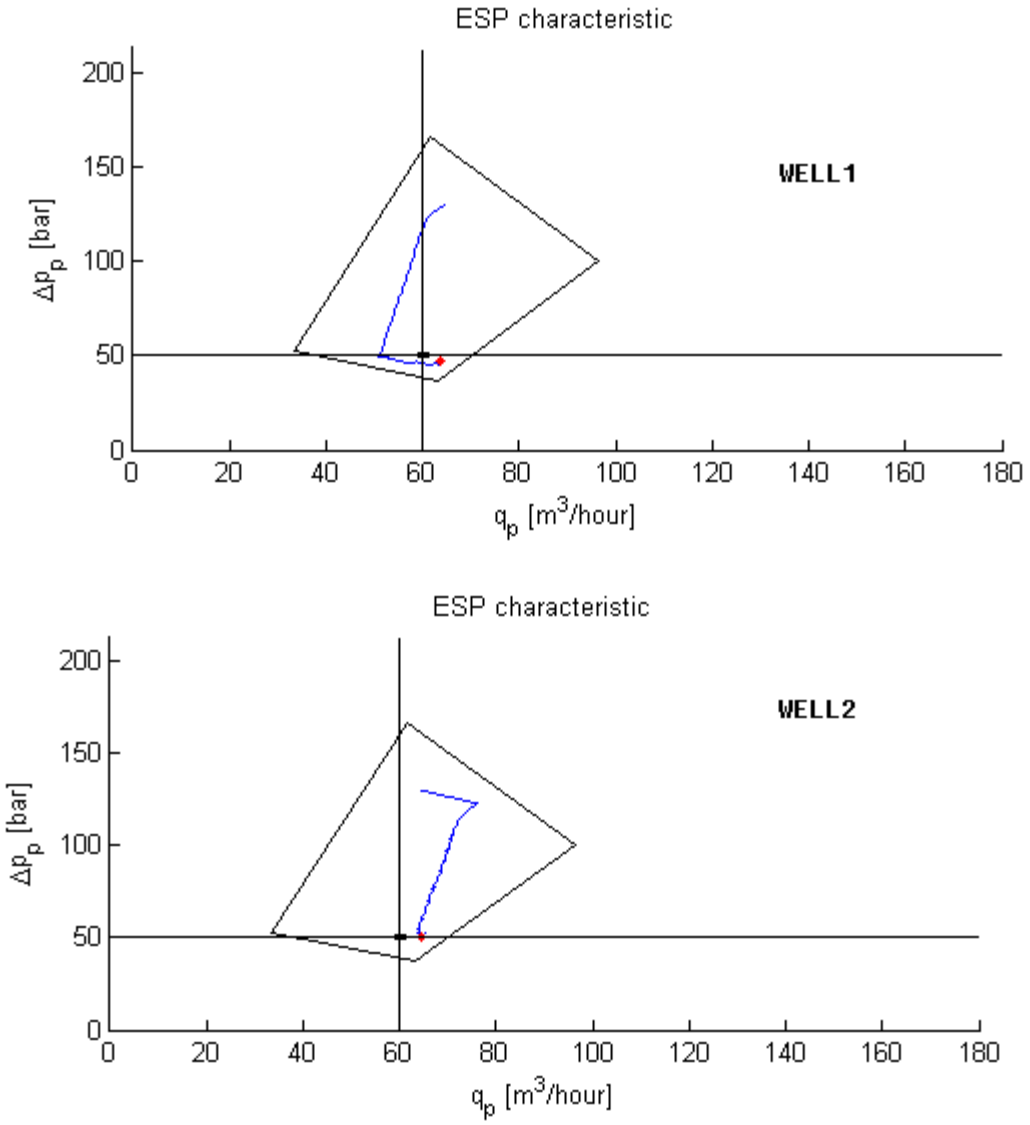

Figure 13 Simulation result of N-wells system

Otherwise, since there are some interactions of the two wells, it is easier for one well to reach the safe region when the other is working. And the region control function still works. This situation showed in

Figure 14.

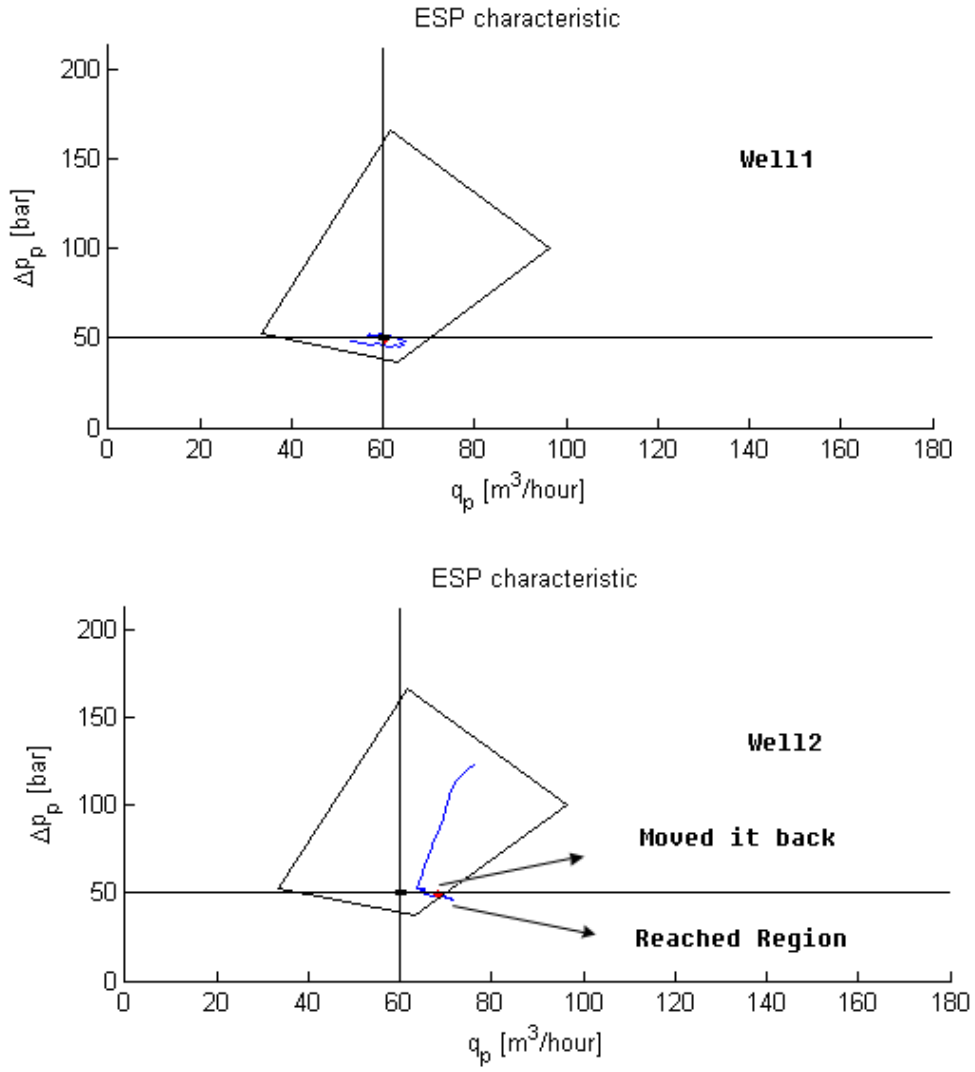

Warning in command window

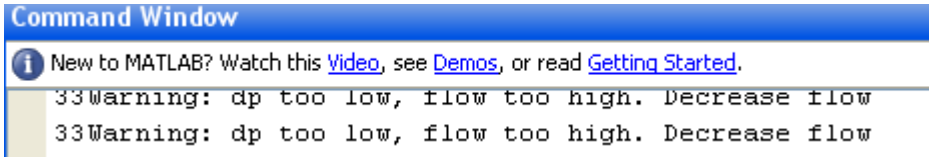

Figure 14 Simulation of region control for N-wells system

9 Data analysis of the SIRI-well

It is necessary to get reasonable values for the constants in the models and to compare the simulation results with data from a real well. Therefore the SIRI production data from

the 18th and19th of December 2009 were used and the relevant information extracted. The program used to carry out this analysis is located in the folder “Data analysis”.

9.1 Well specific data

The available data for the geometry of the well and all fixed parameters are given in the table below. The ESP position can be extracted from the pressure plot in the SIRI article [4] and from the well geometry. Since only the coordinates of the pipe ends are known it is difficult to say at which end the ESP is located. This uncertainty has a large impact on the interpretation of the data as will be discussed later. Additionally the length of the ESP itself and the exact positions of the pressure sensors are not known which leads to further uncertainties.

Parameters	Value
$h_{waterdepth}$	100 m
h_c	126 mTVD msl
$h_p^{geometry}$	822/930 mTVD msl
$h_p^{article}$	875 mTVD msl
h_r	1020 mTVD msl
ρ	984 kg/m^3
r_1	0.0295m
$r_{1,2}$	0.085 m
μ_1 (live oil)	0.3-0.32 $Pa \cdot s$
μ_2 (dead oil)	4-40 $Pa \cdot s$
p_r	~98 bar

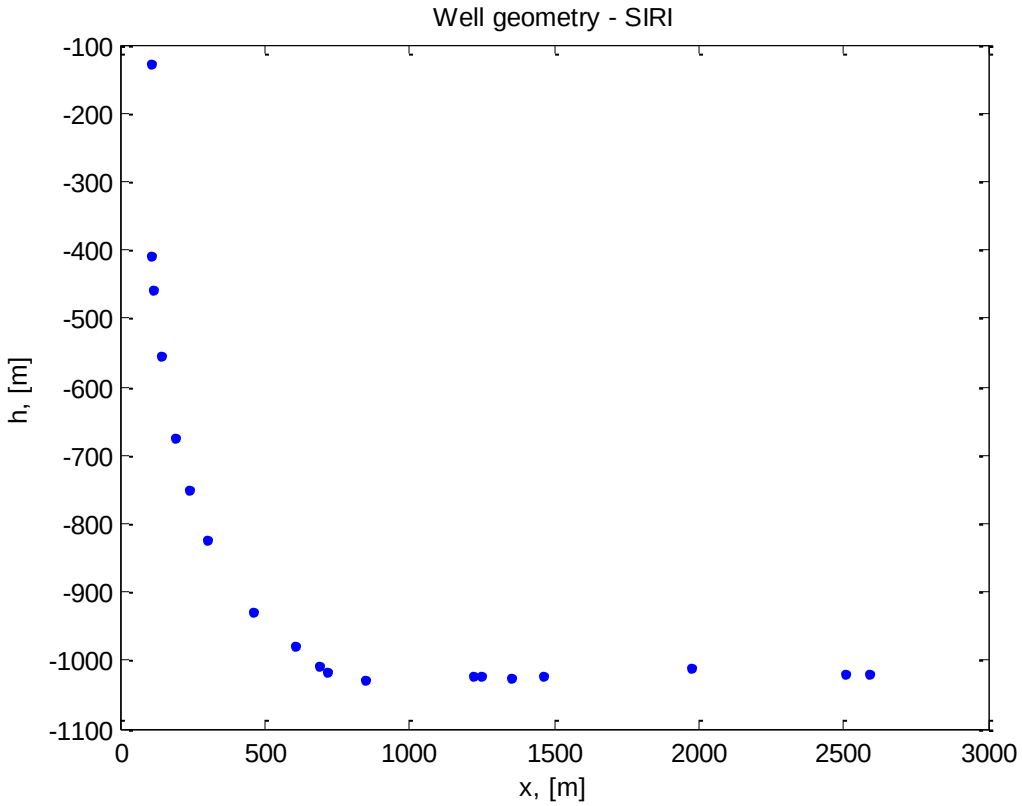

The SIRI well geometry is shown in the figure above. There is a change in pipe-diameter at 1009m TVD from r_1 to $r_{1,2}$. The values for the viscosity are assumed to be constant in each pipe. The change is supposed to take into account that there is or could be a gas separator before the pump. Unfortunately there is no data available about the densities in the different tubes which will also be discussed later. The uncertainty of the reservoir pressure is unknown.

9.2 Field data from SIRI

The production data contain measurements for several system variables, i.e.

System variable	Tag number
p_c^{out}	20-PI-0001
p_c^{in}	20-PI-0057
p_p^{out}	13-PI-3501
p_p^{in}	13-PI-3511
p_{FBHP}	13-PI-3500
$q_{Seperator}$	20-FI-0004 + 20-FI-005
f_p	13-SI-3501

During the measurements of the production data from SIRI the ESP was shut down twice. Before the first shutdown and some time after the second shutdown the observed variables show stable behaviour on slightly different levels. Therefore the system is assumed to be in a steady state within three periods of the whole observation time.

1st steady state	10 – 200 min
2nd steady state	750 – 1400 min
3rd steady state	1600 – 2000 min

In the plot below the measured electrical frequency of the ESP motor is shown for the whole measurement period.

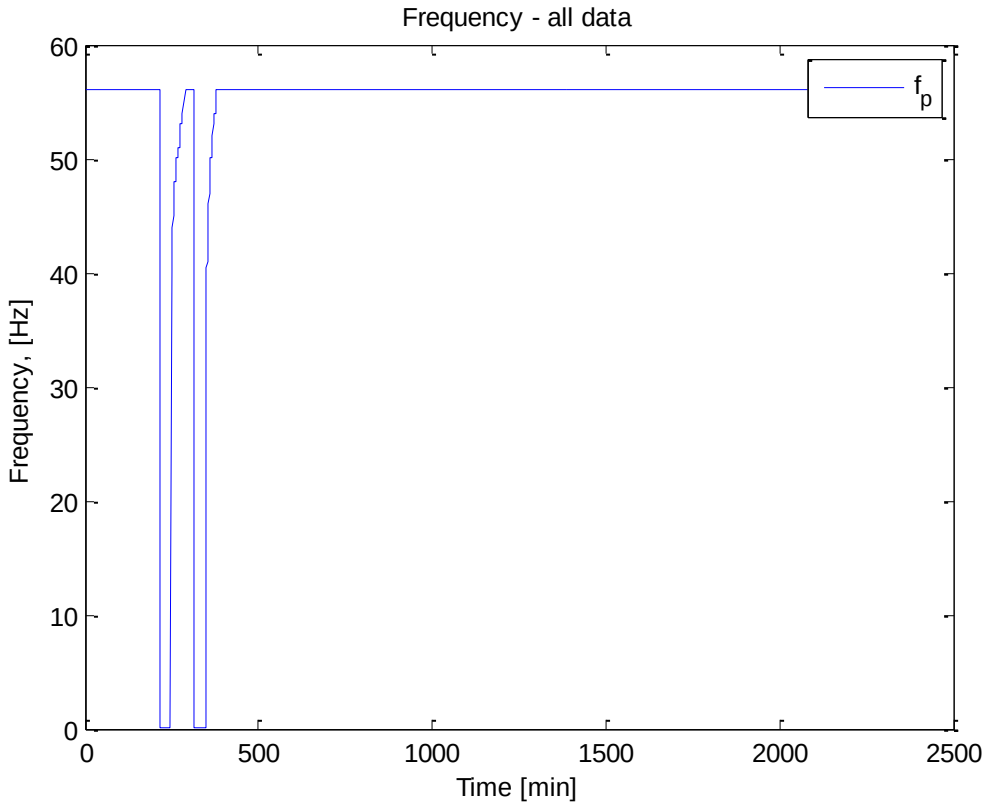

The flow is only measured after the separator, and there separately for oil and water. As one can see in the figure below there are no measurements for the water flow until approximately 1550 min so that it is necessary to make an assumption to find a corrected total flow rate for the whole period.

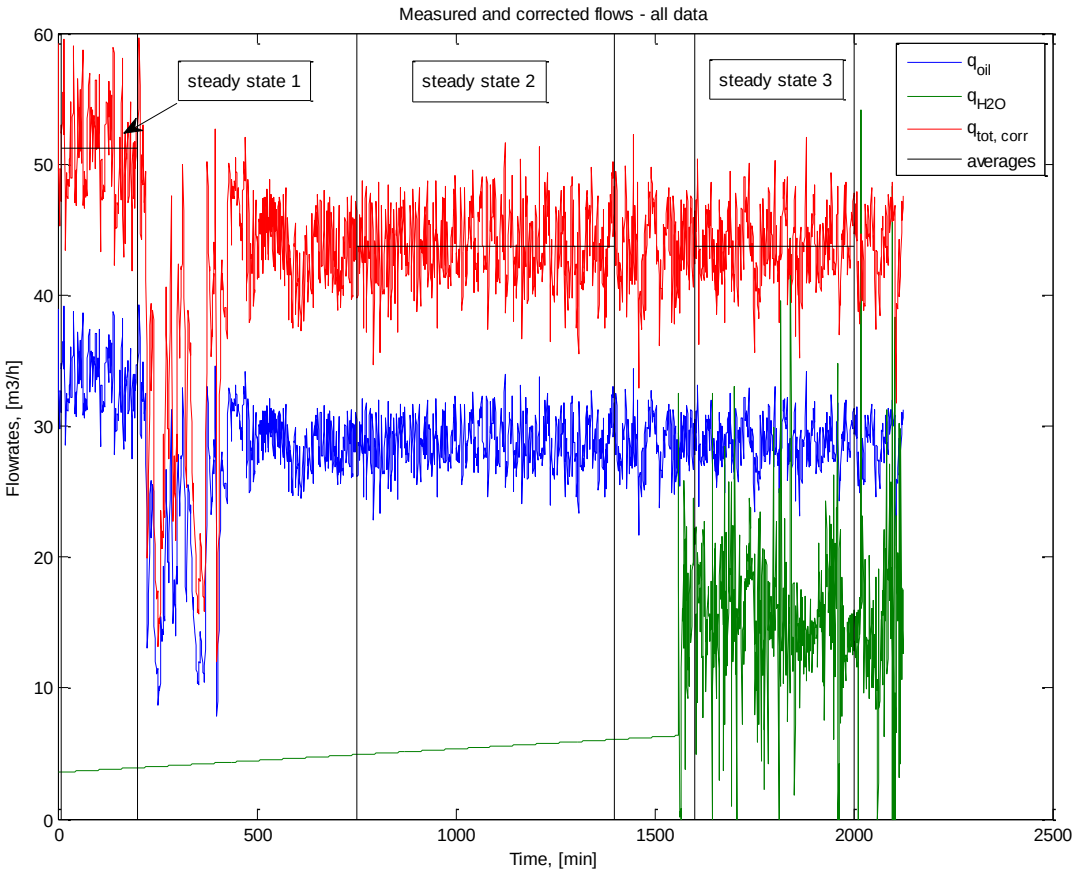

The data available for the 3rd steady state indicate a watercut of about 34 percent.

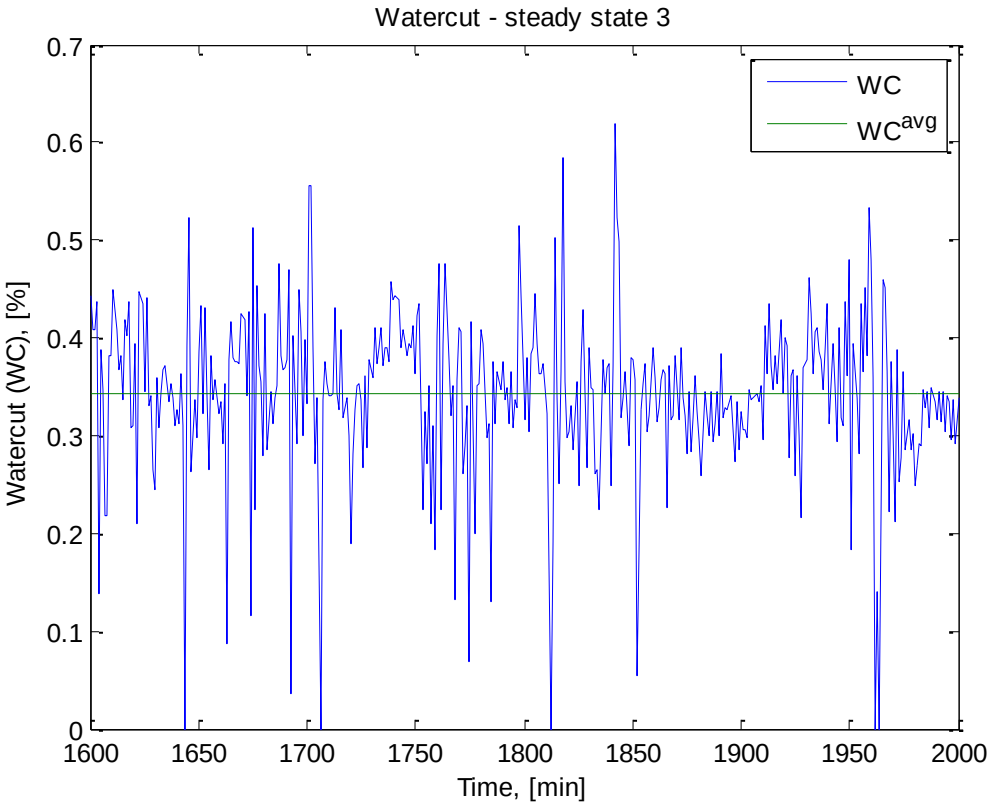

In order to get values for the other 2 steady states the total flow is estimated by assuming a constant watercut for the whole period. The total flow dependent on the oil flow is then given by:

$$q_{tot} = q_{H2O} + q_{oil} = q_{oil} \cdot \frac{WC}{1 - WC}$$

The physical error made by this assumption is difficult to estimate since any possible change of fluid properties due to the shut down is neglected. The mathematical error can be calculated for the 3rd steady state as shown in the figure below.

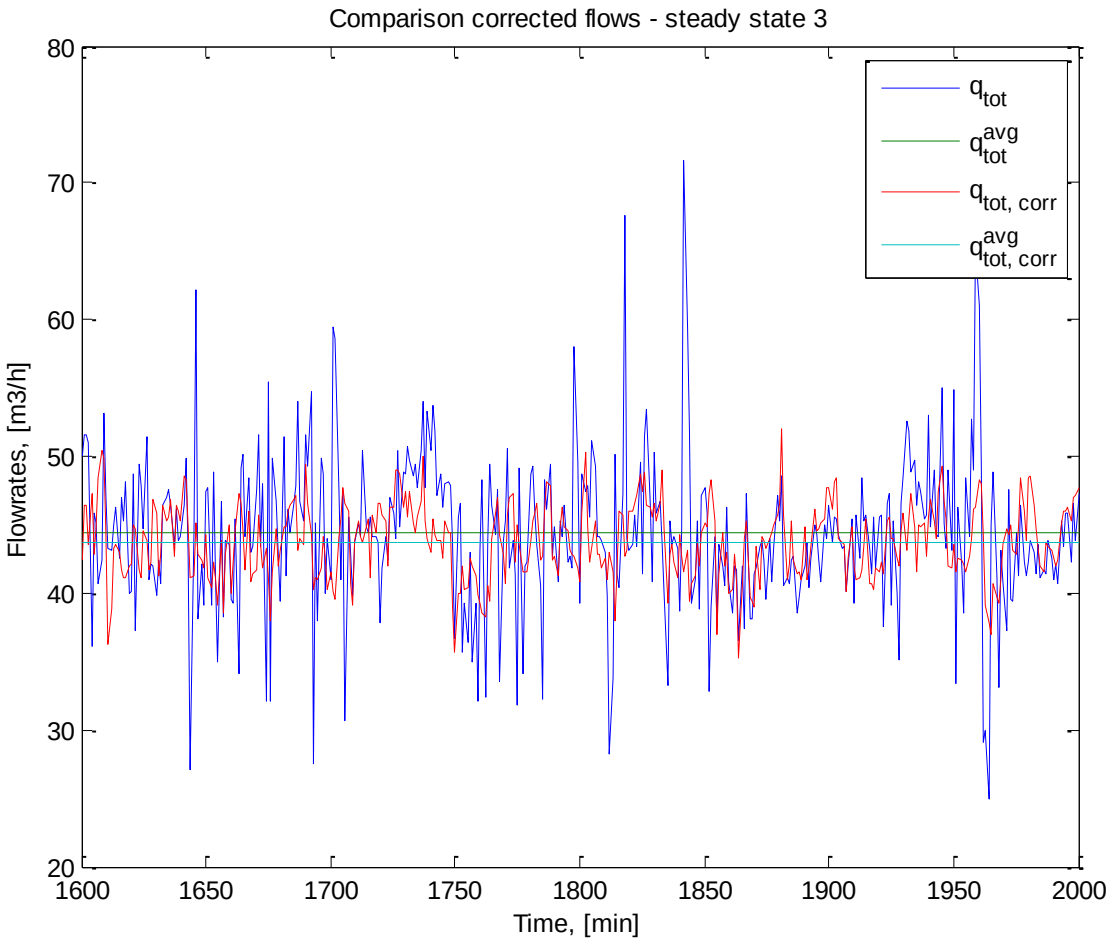

Compared to the oscillations this error is negligible small. The original data contain also highly negative water flows which where set equal zero in this calculation. These data could either be incorrect measurements or be the result of processes in the separator. Anyway the huge relative errors of about 8 to 10 percent make the further analysis difficult since all insights gained will contain a high degree of uncertainty.

The relevant pressures and their change in time are shown in the following plot.

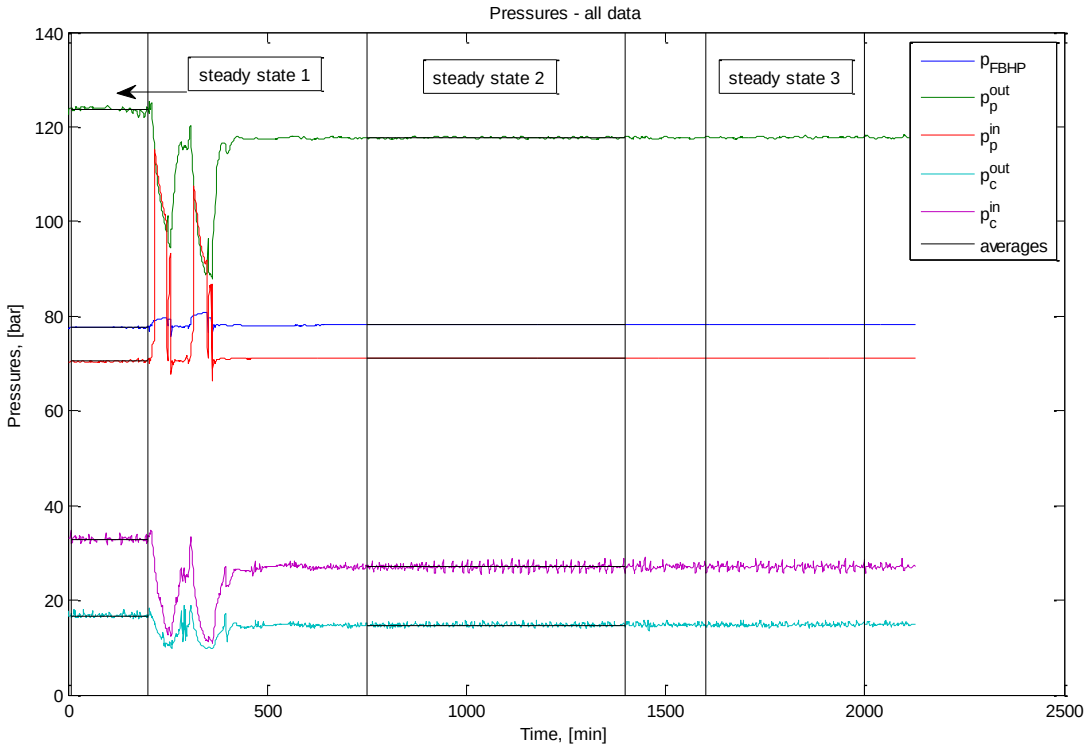

In order to get the needed values for the system states in a steady state the averages and standard deviations of these datasets have been calculated as listed in the table below.

	Tag number	Steady state 1	Steady state 2	Steady state 3
p_c^{out}	20-PI-0001	16.8(4) bar	14.8(4) bar	14.8(4) bar
p_c^{in}	20-PI-0057	32.9(5) bar	27.0(6) bar	27.1(5) bar
p_p^{out}	13-PI-3501	123.8(5) bar	117.7(2) bar	117.8(2) bar
p_p^{in}	13-PI-3511	71.07(3) bar	70.5(2) bar	71.10(3) bar
p_{FBHP}	13-PI-3500	77.57(6) bar	78.14(2) bar	78.17(4) bar
q	20-FI-0004 20-FI-005	51(4) m^3/h	44(3) m^3/h	44(3) m^3/h
f_p	13-SI-3501	56.004(8) Hz	56.00(1) Hz	56.00(1) Hz
WC		34 (9) %	34(9) %	34(9) %

9.3 Data analysis and discussion

9.3.1 ESP frequency

The ESP frequency data show almost constant behaviour. Though this it is not the mechanical frequency but the measured electrical one. One explanation for the differences in steady states could be a deviation between the mechanical frequency before and after the shutdown. Such a deviation might result from a tolerance in the ESP-control which could have a magnitude of 1Hz. Since there is no data available about the ESP used and its characteristics the effect of such a deviation in frequency on the head output cannot be quantified.

9.3.2 Pressures

The pressure measurements show larger variances but compared to the flow data these are negligible. The average values of the first and the other steady states differ to an extend which cannot be explained only by the variance. Since the steady states are not the same, apparently something in the system is different. This might be the mechanical ESP frequency as discussed above. Another possible explanation could be a choke opening somewhere in the system. Physically a shutdown shout result in a separation of the different phases of the fluid, i.e. there are different layers of gas, water and oil which should lead to different measurements during the start-up phase. Eventually, the original fluid properties should be reached which ceteris paribus should lead to the same steady state. This is apparently not the case. Therefore at present there is not a single explanation of this behaviour, but only assumptions or possible explanations. As discussed in the section about the transition states the data indicate a behaviour which need an exhaustive analysis and more information about the actual system setup.

9.3.3 Flows

In order to obtain the remaining parameters e.g. the PI constant or the choke constant the flows at these points in the system are needed. In a steady state the flow in the whole system should be constant which makes it possible to use the flow data available after the separator to determine these constants. Due to the huge oscillations in the flow data which might be caused by a control system for the separator, the huge relative error of the flow data affects the determined constants. This reduces the quality of possible observations. Nevertheless the measured pressures do not show related oscillations which indicates a quite stable steady flow. Assuming that the total production over such a large period can be extracted from the separator more exactly, the constant pressure data suggest a smaller error for the average flow as the statistical analysis implicates.

9.3.4 Determination of system parameters

Since there is no information given about the degree of choke opening it is assumed to be constant over the whole measurement period and set to 100%. With a given flow and pressure difference all constants can be determined using the data of one steady state, e.g. the first one.

K_c	$212\,(19) \cdot l \cdot \sqrt{bar}\ / \min$
$n - stages$	24.5
PI	$6.96\,(51) \cdot 10^{-9}\, m^3\,/(Pa \cdot s)$

As will be discussed below, only the data from the steady states can be used to determine the constants. This restricts the adaption of the ESP-characteristics to only one working point, i.e. the number of stages can be used to obtain the same behaviour at that point, thus further adaption of the characteristics is not possible. Since the number of stages actually can only be an integer value, this adaption could also be achieved by introducing another scaling factor in head-axis of the characteristics. This was not done here since this additional degree of freedom only makes sense if the actual number of stages is known. Since neither the actual characteristics nor their dependency on watercut or viscosity are given for this experiment, at present an additional degree of freedom would not entail more insights. As discussed in the ESP-chapter it is possible to refine the model of the ESP to take all these variables into account at which this only makes sense if there are data available to cross check the model.

9.4 Comparison to the simulation results

Most variables of the simulation can be determined or approximated from the field data, but some degrees of freedom remain, e.g. the density in the first pipe. The figure below shows the pressure profiles in steady state of the complex model with m = n = 100 control volumes for the different ESP-positions assuming the same density in both pipes. Additionally the field data for the first steady state are marked with points. As one can see the simulation results are not the same and do not agree with the field data.

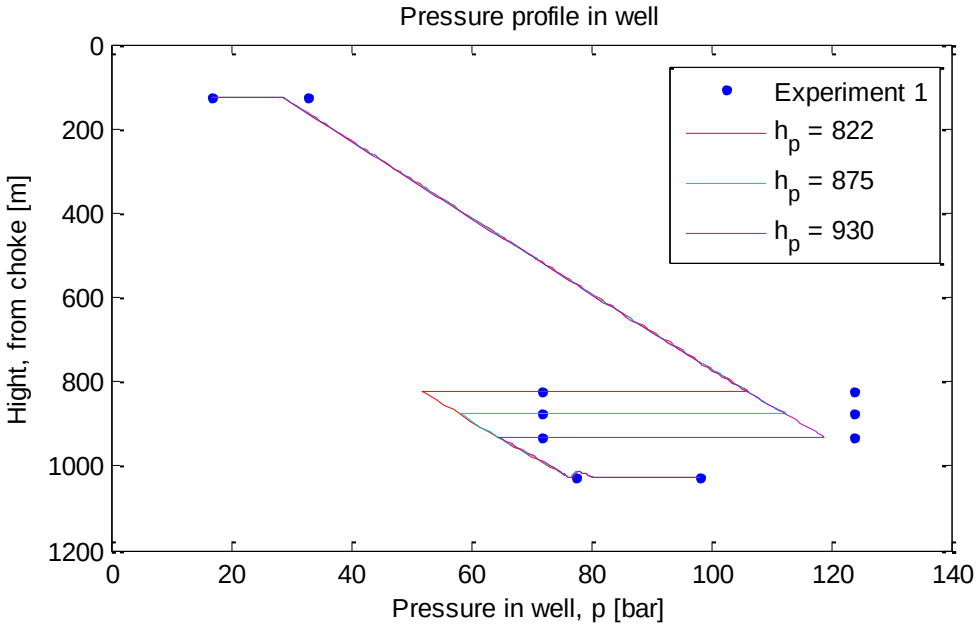

The simulation flows are within the interval 43.97-44.32 m^3/h which is much lower than the 51(4) m^3/h given in the field data. This means, that the overall pressure drop is too high which could be caused by too high friction. In the first tube the measured pressure drop is much lower than the simulated one. In fact it is even smaller than the hydrostatical pressure drop in the assumed well geometry which indicates that there is some inconsistency in the data instead of an error in the simulation. This observation can be explained by two different effects. The hydrostatical pressure drop is dependent on the height and the density. As already stated the density in the first pipe before the gas separator is not known and assumed to be the same as of dead oil after the pump. This might not be completely correct, but the density needed in order to reproduce the same pressure drop would be around 500 kg/m^3 which is far to small. This suggests that there has to be an additional contribution which could be the height. The position of the ESP is not known precisely and as shown in the figure the differences are significant. Since the exact position of the pressure sensors are not known either it might be possible that the flow bottom hole pressure is not measured at the end of the well as assumed in the model interpretation of the data but somewhere between the reservoir and the pump. Thus the hydrostatical pressure drop would be lower as indicated by the data. The additional hydrostatic pressure drop after the flow bottom hole pressure sensor would then be omitted and would not affect the result since it would not contribute in the reservoir model.

The uncertainty in the sensor positions makes it difficult to verify the friction model against the data provided. The hydrostatical and the frictional pressure drop cannot be separated precisely. Though it is possible to compare the simulated friction to the friction for different pump heights. This rough comparison shows that the magnitude is correct.

For a better proof or a better matching between model an reality an empirical friction function might give better comparisons. Therefore the transition states were examined.

It can be stated that it is possible to adapt the parameters of the model in a way to reproduce the field data exactly, but this adaption does not give further insights into the accuracy of the model due to the large uncertainties in the data available. At present it is not in the scope of this project to work on a better match of the simulation data to the field data available. Once the simulation is to be applied to a Statoil operated well, the efforts needed for this matching can be taken. Though data quality and quantity should be improved.

9.5 Transition states

In order to separate the hydrostatical and the friction contribution to the pressure drop in the well it is necessary to obtain data for different pressure drop-flow combinations. This is possible within different steady states or in a very rough approximation also within the transition states between the shut-down and start-up. Unfortunately there are only two steady states available which is too small to obtain an empirical friction function. Additionally the two steady states are quite similar and the origin of the difference between them is not known at present. Therefore the needed data might be extracted from the transition states.

The measured pressures in the transition states between min 200 and 450 are shown in the plot below.

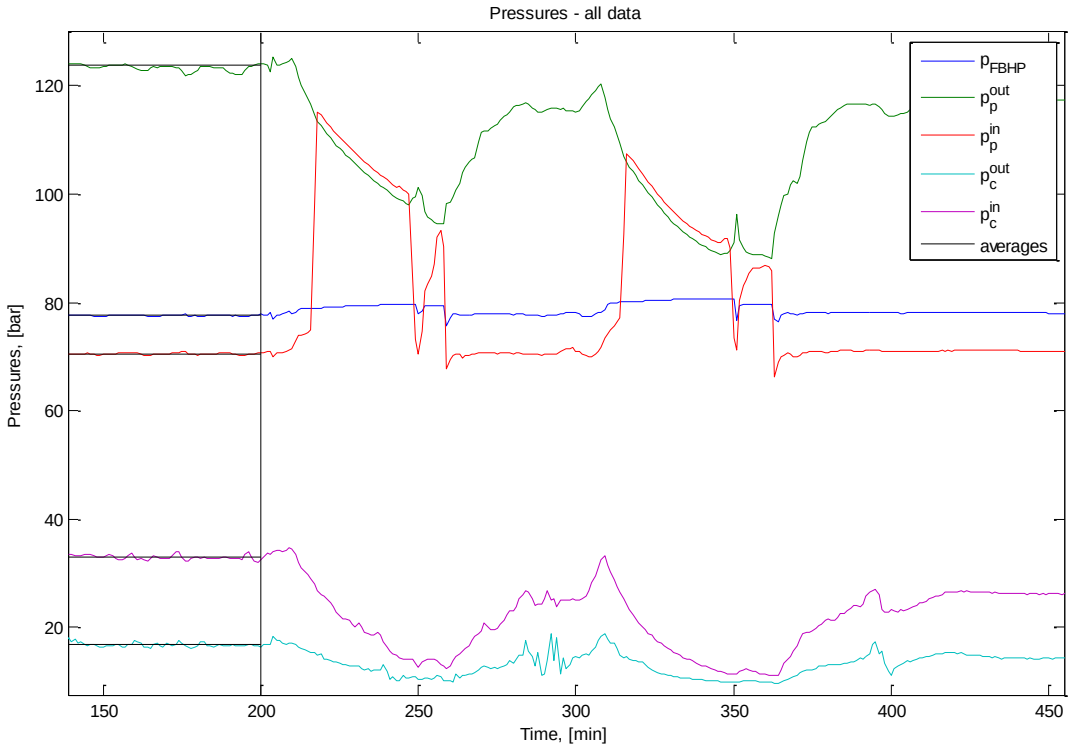

When the ESP is shut down the pump output pressure p_p^{out} as well as the choke pressures p_c^{in} and p_c^{out} drop to some extent as one might intuitively expect. The flow bottom hole pressure p_{FBHP} and the pump input pressure are increasing, which can be explained by the increasing hydrostatical pressure.

Several things can be noted:

- The pressure difference at the choke stays positive over the whole period which suggests that there is outflow or no flow but at least no backflow.
- The pressure difference at the ESP changes sign, which suggests that the ESP is completely shut down. The pressure difference of about 2 bar has a hydrostatic component, which, using the approximate density, indicates a distance of about 20m height between the pressure sensors at the inlet and outlet. Additionally there might also be a contribution due to friction if there still was a flow. From this information only the sign of the flow cannot be determined.
- The measured oil flow after the separator apperars reacts without a large delay. This supports the assumption that the measured flow data can be used to obtain the steady state flow. The flow stays positive, which either might result because of the delay or additional sources, e.g. other wells.

- The pressures measured at the pump and at the choke show a falling behaviour and do not stabilize before the ESP is turned on again. This decrease can be explained either by a decreasing input pressure into the system or by a net outflow.
- Surprisingly the flow bottom hole pressure does not increase to the same extent as the pump inlet pressure does. In fact it almost stays constant and is lower than the pump intake pressure though the hydrostatic contribution should be larger. An approximated hydrostatic pressure increase between the pump and the reservoir suggests a higher flow bottom hole pressure than reservoir pressure.

The latter would lead to a backflow through the choke into the reservoir which is not the case as indicated by the first observation. Therefore this behaviour can only be explained by assuming an additional contribution, e.g. a choke between the ESP and the reservoir.

9.6 Unknown system parameters

If such a choke existed and was closed in parallel to the shutdown of the ESP, the hydrostatic pressure increase due to reduced pump power would only affect the sensors downstream this choke, i.e. the ESP pressure sensors. The flow bottom hole pressure would be increasing to some extent until an equilibrium with the reservoir pressure was reached. These two conclusions fit exactly to the observations made.

The positive sign of the choke flow at the top is difficult to fit into the picture:

If the topside choke was closed, the pressure difference at the choke would stay constant. Since the pressure in the second tube is still decreasing there has to be a net outflow. This outflow could e.g. arise due to leakage which would not explain the decrease in the choke downstream pressure. Since the flow out of the well would be zero, the measured flow at the separator would have to be explained by other sources, e.g. other wells if the topside choke was installed at a manifold instead of the top of one single well.

If the topside choke was open the positive pressure difference indicated an outflow out of the second tube. This outflow could explain the occurring pressure decrease. Since the observed period is several minutes the net outflow can only be a possible explanation if the topside choke is assumed to be almost closed. Otherwise the pressure would decrease much faster. Another possible explanation is another source of flow between the closed choke upstream the ESP and the topside choke, e.g. leakage.

Looking at these different possibilities it is difficult to determine what really is going on. As discussed in the section about start-up and negative pressures there might be additional contributions due to a gas phase if the fluid level sinks in the second tube, e.g. caused by a pressure drop below the bubble point.

It can be stated that the data show a behaviour which suggests the existence of unknown system parameters, e.g. the discussed choke. Therefore it is not possible to use the data from the transition states for further model analysis as long as the contribution of this unknown factor is not clear.

The original goal of this analysis was to obtain an empirical friction function. This could have been done by assuming that e.g. the choke model for a steady state can be applied though there is transition behaviour. The measured pressure differences at the choke could give riese to estimated choke flows such that the needed flow-pressure drop data sets could be obtained. Since, as stated above, the system behaviour cannot be completely explained this calculation is not meaningful. Therefore the extraction of an empirical friction function is not possible at present.

10 Summary and conclusion

In this summer project a first prototype of an automated control system for ESP lifted well systems was developed and implemented. Therefore several physical models with different complexities, both static and dynamic, were developed. The model accuracies were analysed with respect to numerical aspects and compared to field data from the SIRI experiment. The automatic control system was tested in different scenarios and the results were discussed.

Due to lack of time it was not possible to integrate the complex model in the implementation of the N-wells system. Additionally the control of the manifold components was not implemented since as discussed the modelling of the booster pump requires additional efforts.

From the physical point of view the developed models can or should be verified against better field data to gain more insights in the actual accuracy. Due to the modularized implementation it is easy to implement more sophisticated models for the different parts as e.g. the ESP or the reservoir. If the model should take more fluid properties into account, the used differential equations might need to be corrected. E.g. in the case of different densities or a multiphase flow the model has to be extended. The implementation of e.g. temperature or water cut dependency of the viscosity should be straight forward.

For the purpose of controller design the provided system should fulfil all requirements. Only the manifold and the booster pump should be modelled in a more sophisticated way since e.g. the water valve will lead to different fluid properties (change in water cut).

All in all we were able to achieve almost all specifications and want to thank our supervisors Vidar Alstad and Alexey Pavlov for their support and patience.

A Appendix

A.1 Bibliography

- [1] Frank M. White, *Fluid Mechanics.*
  McGraw-Hill Book Co., International Editions 1994.
- [2] Glenn-Ole Kaasa, *A simple dynamic model of drilling suited for control designs*.
  Research Centre Porsgrunn.
- [3] Olav Egeland and Jan Tommy Gravdahl, *Modeling and Simulation for Automatic Control*.
  Marince Cybernetics, Second edition June 2003.
- [4] *Siri Pilot Project – Frist Offshore Extra Heavy and Viscous Oil Ever Produced.*
  Offshore Technology Conference
- [5] Gabor Takacs, Ph.D, Electrical *Submersible pumps manual: Design, operations, and maintenance.*
  Elsevier Inc., 2009.

B Program descriptions

B.1 General program description

Here, a general description of the purpose of the functions in the different program folders will be given. For more detailed information on what specific functions do, see the header comments in the specific functions.

B.1.1 The one well program: Artificial lift models

The program for the single well is divided into several subfolders:

- Complex model: All functions specific to the complex model are contained in this folder. That includes differential equations, calculation of steady state and initial condition.
- Control: All control specific functions are located in this folder. That includes choke and ESP controllers (PI controllers), quantizers, transition calculation functions and the region control function. The over all control function, called `combinedControl.m` is also located in this folder.
- GUI: GUI specific functions and figures are contained in this folder. In addition, the function discarding and plotting data is located here.
- Modules: General functions needed by both models are located in this folder. That includes the ESP and choke characteristics.
- Parameters: This folder contains functions where physical constants and information about well geometry are stored. All physical constants are hard coded in the function `parameters.m`.
- Simple model: This models contains the exact same functions as the folder "Complex model", but modified for the simple model.

B.1.2 Multiple wells program: Artificial lift models N wells

The program for N wells is divided into several subfolders:

- Control: Contains the quantizer and transition functions for the water valve and the booster pump. The combined control function for the N wells is also included here, and this function needs the ESP and choke control related functions from the one well program.
- GUI: The GUI for the N wells model is located here. In addition, the functions for deleting data and plotting figures are located in this folder.

- Modules: The booster pump function is located in this folder.
- Parameters: All the parameters used by the N wells program is stored in functions in this folder. The function `NwellsSystemParameters.m` contains parameters general for the hole system and for the manifold, and the function `NwellsWellParameters.m` contains all well specific parameters. The well geometries for all the wells are also located in this folder.
- Simple model: This folder contains the functions specific to the simple model of the N wells system. That includes the differential equations and the calculation of steady state and initial condition.

B.2 Calculation and changing of the ESP characteristics

The ESP functions are located in the "Modules" subdirectory of the single well folder. The `dpESP.m` and the `qESP.m` function each have their own characteristics function which is called `dpESPcharacteristics.m` and `qESPcharacteristics.m` respectively. In those files the polynomial coefficients are stored hard coded. If the characteristics are to be changed, these files have to be changed. ESP characteristic polynomial calculation is done in the `calculateESPcharacteristics.m` file. The file has two cells. The first one is only to prove the affinity laws. In the second one the data for one pump model for different water cuts are stored hard coded in SI units. The degree of the polynomial can be determined using the variables `degree_hq` for the polynomial flow as a function of head and `degree_qh` for the polynomial head as a function of flow. The output in the MATLAB window than has to be copied to the `dp/qESPcharacteristics.m` function. Additionally the degree in those functions has to be updated.

B.3 Calculation and changing of the choke characteristics

The choke characteristics can easily be changed by changing the function `chokeCharacteristic.m` in the folder "Modules". Data points for the function $G(z_c)$ are hard coded in this file, and interpolation is used to evaluate the function between data points.

As discussed earlier, the interpolation function is slow, so if increased performance is desired, the interpolation can be replaced by a fitted polynomial. However, his causes the choke characteristics function to become negative for small choke openings. To correct this, more data points were created between the data points for the to smallest choke openings by linear interpolation. This corrected the problem, but the behaviour of the fitted polynomial is not good for small choke openings. The choke characteristics and the fitted polynomial are shown in Figure 16, and the code used to make this figure is given in the `chokeCharacteristic.m` function. Use of the polynomial instead of interpolation is implemented and can be commented in if desired.

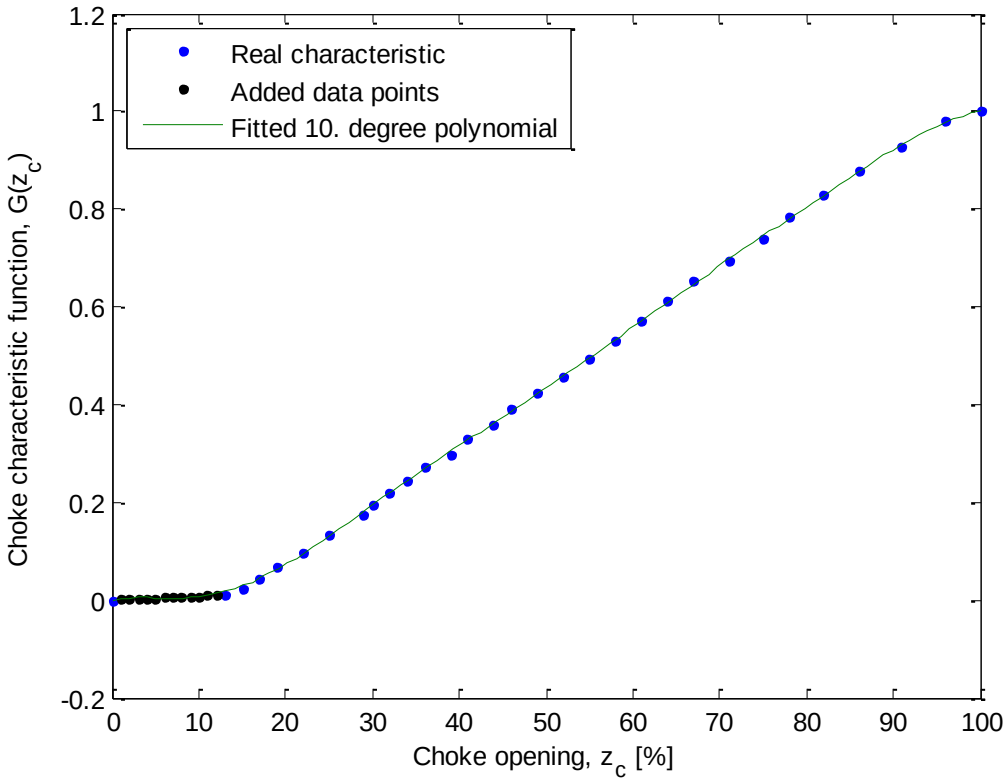

Figure 16: This figure illustrates the attempt to fit the choke characteristics with a 10. degree polynomial to increase the performance of the program. For small choke openings, this is not a good approximation.

B.4 Changing the well geometry

The geometry of the well, given as (x, y) data points is hard coded in the file `calculateWellGeometry.m` which is located in the folder "Parameters" in the program folder for the single well. To change the well geometry this functions has to be altered. At present, to different well geometries are implemented. To switch between the two different geometries, just comment in/out the desired parts.